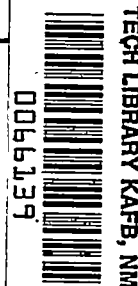


9327 7206 NT VCA



# NATIONAL ADVISORY COMMITTEE FOR AERONAUTICS

TECHNICAL NOTE 3024

MAXIMUM EVAPORATION RATES OF WATER DROPLETS  
APPROACHING OBSTACLES IN THE ATMOSPHERE  
UNDER ICING CONDITIONS

By Herman H. Lowell

Lewis Flight Propulsion Laboratory  
Cleveland, Ohio



Washington

October 1953

AFMDC  
TECHNICAL LIBRARY  
AFL 2011



## NATIONAL ADVISORY COMMITTEE FOR AERONAUTICS

## TECHNICAL NOTE 3024

## MAXIMUM EVAPORATION RATES OF WATER DROPLETS APPROACHING

## OBSTACLES IN THE ATMOSPHERE UNDER ICING CONDITIONS

By Herman H. Lowell

## SUMMARY

When a closed body or a duct envelope moves through the atmosphere, air pressure and temperature rises occur ahead of the body or, under ram conditions, within the duct. If cloud water droplets are encountered, droplet evaporation will result because of the air-temperature rise and the relative velocity between the droplet and stagnating air. It is shown that the solution of the steady-state psychrometric equation provides evaporation rates which are the maximum possible when droplets are entrained in air moving along stagnation lines under such conditions. Calculations are made for a wide variety of water droplet diameters, ambient conditions, and flight Mach numbers. Droplet diameter, body size, and Mach number effects are found to predominate, whereas wide variation in ambient conditions are of relatively small significance in the determination of evaporation rates.

The results are essentially exact for the case of movement of droplets having diameters smaller than about 30 microns along relatively long ducts (length at least several feet) or toward large obstacles (wings), since disequilibrium effects are then of little significance. Mass losses in the case of movement within ducts will often be significant fractions (one-fifth to one-half) of original droplet masses, while very small droplets within ducts will often disappear even though the entraining air is not fully stagnated. Wing-approach evaporation losses will usually be of the order of several percent of original droplet masses.

Two numerical examples are given of the determination of local evaporation rates and total mass losses in cases involving cloud droplets approaching circular cylinders along stagnation lines. The cylinders chosen were of 3.95-inch (10.0+ cm) diameter and 39.5-inch (100+ cm) diameter. The smaller is representative of icing-rate measurement cylinders, while with the larger will be associated an air-flow field similar to that ahead of an airfoil having a leading-edge radius comparable with that of the cylinder. It is found that the losses are less than 5 percent. It is concluded that such losses are, in general, very small.

2734

T-10

(less than 1 percent) in the case of smaller obstacles (of icing-rate-measurement-cylinder size); the motional dynamics are such, however, that exceptions will occur by reason of failure of very small droplets (moving along stagnation lines) to impinge upon obstacle surfaces. In such cases, the droplets will evaporate completely.

## INTRODUCTION

Several studies (for example, refs. 1, 2, and 3) have recently been made of trajectories of water droplets entrained in atmospheric air approaching wings or liquid-water-content measurement cylinders. In these trajectory studies it has been assumed that the droplet shape and mass remain unchanged despite possibilities of deformation and evaporation arising in connection with the presence of local compressible flow fields in the vicinity of wing or cylinder. In such fields, air temperatures and pressures are no longer those of the undisturbed stream. Moreover, the droplet acquires, in general, a velocity with respect to the disturbed air.

In view of the air temperature and pressure changes that occur and the existence of an air-droplet relative velocity, it appeared desirable to determine the magnitudes of evaporation mass losses occurring in the vicinity of obstacles or within ducts. The assumption that the droplet remains spherical was retained.

The general literature in the field of evaporation from droplets is extensive, but few studies of the particular problem of droplets approaching obstacle under icing conditions have been made. Both Hardy (ref. 4) and Langmuir (ref. 5) have considered certain aspects of the question; both analyses took into account the fact that the droplet will not, in general, be in instantaneous psychrometric equilibrium with its surroundings. In both cases, the conclusion was reached that total evaporative losses from droplets actually reaching obstacle surfaces are of the order of several percent for the particular sets of conditions of their analyses. In both investigations, however, the ranges of droplet size, air temperature and pressure, body size, and flight Mach number were rather restricted.

A complete treatment of the problem would require:

(1) use of the equations of motion of a droplet of liquid in a (compressible) gas, the equations to take into account in some way changes of drag coefficient with Mach number;

(2) use of the equations governing the dynamic thermal behavior of a volatile sphere under quite general conditions of changing heat and mass-transfer rate including, in some instances, radiation effects; and

(3) coverage of wide ranges of obstacle size and shape, droplet size, flight Mach number, and flight ambient air conditions.

The unavailability of a suitable high-speed calculator made it necessary, however, to restrict in some manner the scope of the calculations.

Since the subject of droplet evaporation, insofar as aircraft are concerned, is of interest chiefly in connection with icing, radiation effects could be ignored (since all temperature levels involved are low).

Further, it was decided to consider that a droplet remains in instantaneous psychrometric equilibrium with its immediate surroundings, and its internal temperature was to be taken as uniform. Certain quantitative aspects of this assumption are scrutinized in the body of the report and in appendix B; a qualitative justification of the procedure is, however, given here.

If evaporation occurs at all, it will occur principally as a result of a droplet temperature rise, with which a droplet-surface vapor-pressure rise will be concomitant. Therefore, maximum evaporation rates will occur, in virtually all cases, in the vicinities of body stagnation points. If, now, bodies and flight conditions (wing attitudes, for example) are considered such that air flows in the vicinities of stagnation points are essentially symmetrical about such points, then the trajectory of a droplet originally on a stagnation line will essentially coincide with the line. For the sake of simplicity, then, let attention be confined to histories of droplets moving along such lines. Air temperature and pressure will rise monotonically. The droplet instantaneous position will always be ahead of that of the air with which, at an arbitrary previous time, it was in contact, although a quasi-static mass-transfer analysis does not demand such motion. More importantly, with or without evaporation the interior droplet temperature will always lag behind the rising surface temperature, and both the mean droplet temperature and the surface temperature will always be less than the local equilibrium (psychrometric) value; all droplet temperatures will rise monotonically. It is possible to conclude that both the actual local time rate of evaporation and the actual total loss of liquid will be less than those calculated on the basis of psychrometric calculations in the case of stagnation streamline droplet motion. It therefore follows that the present quasi-static calculations set upper bounds to the loss rates and total losses for motion along stagnation lines.

Finally, evaporative losses off stagnation streamlines will in general be less than stagnation-streamline values because of the fact that maximum temperature rises occur along the latter.

Accordingly, it is proper to consider that psychrometric-equilibrium calculations establish limiting local (and, when integrated, total) losses

2734

CJ-1 back

which are never exceeded in real situations. Moreover, the results apply without change to the histories of small droplets moving within long ducts or toward large obstacles.

Since the calculations of mass losses are made under the assumption of the existence of successive instantaneous psychrometric-equilibrium states, it is desirable that the degree of quantitative applicability of that procedure be ascertainable in any given case. In the section of the report entitled Response of Sphere to Changes of Environmental Temperature, two parameters are mentioned by the use of which it is possible to assess in a rough manner the degree to which such equilibrium assumption calculations lead to values concordant with mass-loss rates which would be obtained in the case of more rigorous calculations. The expressions determining the magnitudes of the two parameters are derived in appendix B. All symbols used are defined in appendix A.

The detailed calculation procedure used to obtain the mass-loss rates themselves is presented in the section of the report entitled EVAPORATION CALCULATIONS.

The results and possible applications are then discussed; two numerical examples are given. All symbols used are defined in appendix A.

#### General Considerations

The assumption that instantaneous local psychrometric equilibrium exists between droplet and atmosphere eliminates dependency of calculated local loss rate upon previous droplet history. This is true because local droplet calculated temperatures then depend only upon instantaneous local conditions.

When that assumption is made, calculations of maximum possible total mass losses in actual physical situations may be made in the following manner:

Droplet mass-loss rates for reasonable combinations of droplet size, local ambient (relative) conditions, and relative air-droplet speed are calculated; the details of the procedure are given in the section entitled EVAPORATION CALCULATIONS.

The variations of air speed, temperature, and pressure along the forward stagnation line are obtained in some manner for the particular physical situation of interest.

The motional history of a droplet of the size for which the calculations are being made is then obtained for the case of motion essentially along the stagnation line; this was accomplished by the use of a differential analyzer or by the use of some numerical technique. The local

rates of evaporation were then obtained simply by interpolating among the results of the generalized evaporation calculations at reasonable intervals; the tacit additional assumption is made here that the over-all mass loss will be small, so that constancy of droplet size may be assumed to a sufficiently high degree of approximation in making a calculation of local mass-loss rate.

Finally, the over-all mass loss is obtained by adding the small loss increments corresponding to the selected droplet path increments. If the over-all loss is greater than, say, 10 percent, the decrease of droplet size can easily be taken into account.

#### RESPONSE OF SPHERE TO CHANGES OF ENVIRONMENTAL TEMPERATURE

It has been found practicable, in the calculations made in connection with the present study, to cover wide ranges of the several variables involved only because droplet internal temperature uniformity and psychrometric equilibrium with the environment were assumed. These assumptions greatly simplified the calculations while at the same time permitting conclusions to be reached as to limiting evaporation rates in real situations.

It was considered desirable, however, to attempt to establish criteria whereby the degree of departure of equilibrium values of droplet temperature and evaporation rate from actual values could be estimated. While precisely this goal was not attained, criteria were established which serve to determine what might be designated the "degree of invalidity" of the basic equilibrium assumptions.

The criteria themselves are derived in outline form and are discussed in appendix B. It is sufficient here to mention that three variables are of importance in this connection. Two of these are the times required for a sphere to respond to sudden surface and to environmental changes of temperature. The third variable is the "approach period", which is arbitrarily taken as the period required for the droplet, moving at a speed equal to the relative air-obstacle free-stream speed, to move through an approach distance equal to a principal transverse dimension of the obstacle. At the latter distance upstream of the stagnation point, the air-flow characteristics, while still substantially those of the free stream, will have departed by easily measurable fractions from those of the free stream. For example, the stream-obstacle relative Mach number, for a free-stream Mach number of 0.75, is 0.74 at a distance of one radius from a cylinder surface. It follows that the approach period, as here defined, represents in approximate fashion the time during which most of the change of effective droplet environment occurs as the droplet approaches the obstacle.

The two parameters which then determine the degree of invalidity of a quasi-static treatment are any two among the following three: Ratio of internal to external sphere time constant (for response to a sudden surface or environment change, respectively), ratio of internal time constant to approach period, and ratio of external time constant to approach period.

In general, if both the ratios of time constant to approach period are small, a quasi-static (psychrometric-equilibrium, uniform internal sphere temperature) analysis is quantitatively exact. In all other cases, as indicated in appendix B, the situation is complex and does not readily yield to any simple analysis.

In particular, a quasi-static analysis is exact in the case of the approach of smaller droplets (below about 30 microns diameter) to large obstacles (wings) or motion of such droplets within ducts at least several feet in length. In the case of the long duct, in which, except for a region near the mouth, conditions are uniform, total evaporation losses are obtainable directly from the results of calculations made in connection with the present study, as indicated in the section entitled RESULTS AND DISCUSSION.

#### EVAPORATION CALCULATIONS

The basic numerical result required in these studies was the rate of loss of mass of a water droplet of a particular size moving at a prescribed Mach number with respect to air characterized by a specified deceleration from the original free-stream flight speed and by the free-stream temperature and pressure.

As discussed previously, it was assumed that the droplet remained in instantaneous psychrometric equilibrium with its effective environment; the effective environment consisted of the mixture of air and water vapor the local apparent temperature and pressure of which, with respect to the droplet, were assumed to be altered from the true local (static) values by the motion of the droplet with respect to the air. The quantitative nature of the assumed changes is discussed subsequently.

In outline form, the calculation scheme was the following:

Ambient static air temperature  $T_{st,\infty}$ , ambient static air pressure (inclusive of water vapor  $P_{st,\infty}$ ), and flight Mach number  $M_\infty$  were assumed. A deceleration of the air (fig. 1) to a selected relative air-obstacle Mach number  $M_R$  was then assumed, and the increased local air-plus-water-vapor static temperatures and pressures were computed; the change was assumed adiabatic and isentropic. The effective air and

water-vapor temperature and pressures, on the basis of a given air-droplet relative Mach number  $M_r$ , were then calculated.

It was then possible to compute a local relative air-droplet Reynolds number  $Re_r$ , from which heat- and mass-transfer coefficients were obtained.

By using two temperature-range overlapping quadratic approximations for the vapor pressure of water as substitutes for the more accurate exponential expression, it became possible at this point to obtain, beginning with the psychrometric (heat-balance) equation, a quadratic equation in the droplet temperature and other quantities. This equation was then solved for the droplet temperature; the procedure avoids the iterative calculations otherwise required. The computed mass-transfer coefficient and droplet vapor pressure were then used to obtain the required rates of evaporation.

The significant steps of the calculation are given hereinafter with appropriate explanations of symbol meanings and origins of relations where those are not immediately obvious; the fundamental relation is the psychrometric equation

$$(t_{d,e,l} - t_{d,s})h_h = \lambda h_m(p_{d,s} - p_{d,e,l}) \quad (1)$$

which indicates that the droplet temperature assumed a value such that as much heat is removed in unit time by evaporation as is supplied by free or forced convective heat-transfer processes.

The initial steps are required to determine the effective temperature, air pressure, and vapor pressure of the local environment with respect to the droplet.

The static temperature at the instantaneous droplet position (hereafter identified as local) is a function of the air-obstacle relative total temperature and the local air-obstacle relative Mach number:

$$T_{st,l} = T_e \frac{1 + 0.2 M_\infty^2}{1 + 0.2 M_R^2}$$

The mean effective temperature of the environment with respect to the entire droplet is then calculated from the local static temperature and the droplet-air relative Mach number:

$$T_{d,e,l} = T_{st,l} (1 + 0.16 M_T^2)$$



Note that a recovery coefficient of 0.8 is used; this is no more than a representative average figure based on many data reported in the literature.

Implicit in this relation is the concept that the laws governing events occurring at the forward position of the sphere may be applied with little error to the entire sphere. Fortunately, the Reynolds number regime ( $0 \rightarrow 1000$ ) of interest is precisely that in which, for most smooth, regularly shaped bodies, heat losses and mass-transfer rates are much greater over the forward portions of the bodies than over the rear (unpublished interferometric research performed by E. R. G. Eckert at Wright Field indicating that, in the Reynolds number range  $24.5 \leq Re \leq 605$ , front-to-back local Nusselt number ratios are of the order of 3 or 5 to 1; see also refs. 6 and 7). It is therefore permissible to apply the law of variation (of the particular quantity under consideration) for the forward portion to the entire body, although the absolute level (for example, of a heat-transfer coefficient) will be determined by an experiment involving the whole body at some typical Reynolds number.

Insofar as temperature effects are concerned, there will of course be some heat conduction from the front to the rear, but the fact that the film resistance is much higher in the rear will ensure attainment of essentially front-surface effective temperatures.

The local air-droplet relative total pressure is used in the calculation of air-droplet relative Reynolds numbers, and the relative total vapor pressure in the calculation of air-droplet relative vapor pressure. The reason for this, apart from the fact that little evaporation occurs over the rear portion of the droplet, is that it is shown in references 8 (fig. 8) and 9 (table IV, fig. 3) that at Reynolds numbers below about 50 the pressure in the vicinity of the forward stagnation point is substantially higher than "total".

Emphasis is placed on the low Reynolds numbers regime because air-droplet relative Reynolds numbers will, generally, be small for the smaller (say, below 20 microns) droplets, while evaporation rates will be highest for such droplets.

Accordingly, a rough average pressure for the front surface is the total pressure; the final results, in any case, are not critically dependent upon the nature of the laws of pressure variation assumed in these calculations.

The local air-droplet relative total pressure is given by

$$P_{e,l,r} = P_{st,\infty} \frac{(1 + 0.2 M_{\infty}^2)^{7/2} (1 + 0.2 M_T^2)^{7/2}}{(1 + 0.2 M_R^2)^{7/2}}$$

In the calculation of effective local water vapor pressure, it is first necessary to determine the original (static, free-stream) vapor pressure, either complete or 90-percent saturation being assumed.

While it is necessary only to consult a table of values to determine the vapor pressure in question, it was decided that the quadratic relations used subsequently to calculate the saturation vapor pressure at the droplet surface should also be used in other vapor-pressure calculations so as to avoid the small inconsistencies which would otherwise arise.

The vapor pressure in the free stream is given by

$$p_{d,\infty} = \sigma(6136 + 438.7 t_{st,\infty} + 10.69 t_{st,\infty}^2) \quad (2a)$$

for

$$-15^\circ \leq t_{st,\infty} \leq 15^\circ \text{ C}$$

and

$$p_{d,\infty} = \sigma(5288 + 287.7 t_{st,\infty} + 4.3047 t_{st,\infty}^2) \quad (2b)$$

for

$$-30^\circ \text{ C} \leq t_{st,\infty} \leq -8^\circ \text{ C}$$

These relations yield approximately correct values of vapor pressure over the intervals indicated. The accuracy of the second equation is higher over the common interval  $-15^\circ \text{ C} \rightarrow -8^\circ \text{ C}$ ; the errors at various temperatures are listed in table I (for the case  $\sigma = 1$ ). The accepted figures were taken from reference 10.

Although neither of the two vapor pressure - temperature relations used is accurate above  $15^\circ \text{ C}$ , the first one given was used for droplet temperature calculations for droplet temperatures as high as  $25^\circ \text{ C}$ ; the results are merely qualitative in the range  $15^\circ$  to  $25^\circ \text{ C}$ , but are retained for the sake of completeness.

In the calculation of effective local ambient vapor pressure, the assumptions are made that the ratio of vapor to air pressure remains constant and that  $\gamma$  for a mixture of water vapor and air is essentially 1.4.

In connection with the calculation of droplet-air relative Reynolds number, a temperature at which the viscosity is to be evaluated must be selected. The droplet-air relative total temperature

$$T_{d,t,l} = T_{d,e,l} \frac{(1 + 0.2 M_r^2)}{(1 + 0.16 M_r^2)}$$

was selected for that purpose in the earlier stages of the work and subsequently retained for the sake of consistency despite the fact that use of a relative total temperature cannot be justified. The maximum difference between the relative total and relative effective temperatures, however, occurs at  $M_r = 0.75$  (an unusually high figure) and is  $\sim 5^\circ \text{C}$ . The difference between the viscosities corresponding to the two temperatures is then  $\sim 1.5$  percent, while for  $M_r$  values below 0.5 the difference is negligible. Since the viscosity is used only to calculate a droplet-air relative Reynolds number, the effect of any such difference is virtually undetectable.

The droplet-air relative Reynolds number is given by the expression

$$\text{Re}_r = \frac{2\rho_{st,l} r_d V_r}{\mu_t}$$

which is, accordingly, a Reynolds number based upon local static air density, droplet diameter, relative air-droplet speed, and viscosity at  $T_{d,t,l}$ . The viscosity, to avoid irregularities resulting from the use of tabulated experimental values, was obtained from the expression

$$\mu \text{ (poise)} = 10^{-6} [172.81 + 0.48721t - 0.0004932 t^2 + 9.33 \times 10^{-7} t^3]$$

The relation given subsequently between the Nusselt number for heat transfer and the Reynolds number is based primarily on the survey made by Williams (ref. 11). A Prandtl number of 0.73 was used in the calculations. The exponent 0.6393 was selected, in part, because it had previously been found that the drag coefficient of a sphere is given quite accurately over the range  $0 < \text{Re} \leq 800$  by a relation in which that exponent appears; it had therefore been possible, by using that exponent for the heat-transfer equation, to save effort in certain calculations. The expression fits the experimental data well over the range  $0 \leq \text{Re} \leq 10^4$ .

$$\text{Nu}_h = 2.000 + 0.2464 \text{Pr}^{1/3} \text{Re}_r^{0.6393}$$

It should be noted that the assumption has been made, in connection with the expressions for the heat-transfer Nusselt number just given and for the mass-transfer Nusselt number given later, that heat- and mass-transfer processes do not affect each other (except for the establishment of the psychrometric temperature). Otherwise stated, the assumption

is made that the presence of water vapor in the sphere boundary layer does not affect either the inert gas (air) properties or the eddy diffusivity and thermal conductivity. While it is believed that this assumption is valid at low air temperatures and (in particular) at low rates of evaporation, evidence exists tending to invalidate the assumption under other conditions (ref. 12).

The Nusselt number for mass transfer subsequently is somewhat less familiar than  $Nu_h$ ; it is defined as  $(h_m D_d / k_{f,m})$ , where  $h_m$  is the mass-transfer coefficient in  $\text{cm}^{-2} \text{sec}^{-1} (\text{dyne cm}^{-2})^{-1}$  and  $k_m$  is the mass-transfer "conductivity" defined as  $(\rho\beta/P_a)/(M_d/M_a)$ . In the latter,  $\rho$  is the effective medium density,  $\beta$  the diffusion coefficient of the pair of substances, and  $P_a$  a local mean particle pressure of the gas into which the diffusing material is passing (in this case, dry air).

$$Nu_m = 2.000 + 0.330 Re_r^{0.56}$$

The coefficient 0.330 is actually the product of the constant 0.39 and of the selected value of the one-third power of the Schmidt number (0.605) in the expression:

$$Nu_m = 2.000 + 0.39 Sc^{1/3} Re_r^{0.56}$$

The exponent of this relation is that of Williams (ref. 11), while the constant was selected to ensure good fit over the range  $0 \leq Re \leq 3000$ . It will be noted that Williams' data are plotted in terms of the Colburn parameter  $j_m$ , which is defined as follows (note:  $k_{f,m} \equiv (\rho\beta/P_a)(M_d/M_a)$ );

$$\begin{aligned} j_m &= St_m Sc^{2/3} \\ &= \left( \frac{h_m P_a}{G_a} \right) \left( \frac{M_a}{M_d} \right) \left( \frac{\mu}{\rho\beta} \right)^{2/3} \\ &= \left( \frac{h_m D}{k_m} \right) \left( \frac{M_a}{M_d} \right) \left( \frac{k_{f,m} P_a}{\rho^{2/3} \mu^{1/3} \beta^{2/3}} \right) \left( \frac{\mu}{G_a D} \right) \\ &= Nu_m Re^{-1} \left( \frac{\rho\beta}{P_a} \frac{P_a}{\rho^{2/3} \mu^{1/3} \beta^{2/3}} \frac{M_d}{M_a} \right) \left( \frac{M_a}{M_d} \right) \\ &= Nu_m Re^{-1} Sc^{-1/3} \end{aligned}$$

It therefore follows that Nusselt numbers of mass transfer are obtainable from Williams' (and similar) data by multiplying the  $j_m$  values by  $Re Sc^{1/3}$ . Heat-transfer data published since 1942 agree reasonably well with the present empirical equation used herein; mass-transfer data exhibit greater scatter.

It is possible to select a fixed value of Schmidt number because the latter varies rather slowly with both temperature and pressure for rather wide ranges of temperature and pressure in the vicinity of standard atmospheric conditions. It is possible to deduce this slow variation upon inspection of the relation

$$\beta = \beta_0 \left( \frac{T}{273.2} \right)^{1.89} \left( \frac{1,013,250}{P} \right)$$

of page XVI-16 of reference 13. ( $\beta_0$  is  $0.220 \text{ cm}^2/\text{sec}$  at  $0^\circ \text{C}$  for the system water-air, ref. 14.) Since, in the expression  $Sc = \mu_a / \rho_a \beta$ , the viscosity varies roughly as the 0.8 power of the temperature, while air density varies inversely with temperature and directly with pressure, the residual variation of  $Sc$  is a rather slow decrease with temperature.

The psychrometric equation (1), for convenience in discussing the remaining calculations, is now restated in the form

$$t_{d,s} = t_{d,e,l} - X (p_{d,s} - p_{d,e,l})$$

where

$$X = \frac{\lambda h_m}{h_h} = \frac{\lambda k_{f,m} Nu_m}{k_{f,h} Nu_h}$$

The thermal conductivity  $k_{f,h}$  is nearly independent of pressure at moderate pressures, whereas  $k_{f,m}$  may be written

$$k_{f,m} = (k_{f,m})_{N.P.} (N.P./P)$$

In this instant,  $P = P_{e,l,r}$ . The quantity  $X$  may now be expressed as follows:

$$X = \frac{\lambda Nu_m}{Nu_h} \left( \frac{k_{f,m}}{k_{f,h}} \right)_{N.P.} \left( \frac{1,013,250}{P_{e,l,r}} \right)$$

Further, the quantity  $(k_{f,m}/k_{f,h})_{N.P.}$  increases only about 0.11 percent per  $^{\circ}\text{C}$  increase of temperature at  $0^{\circ}\text{C}$ . For present purposes, therefore, the expression

$$\lambda(N.P.) (k_{f,m}/k_{f,h})_{N.P., \text{ fixed temperature}}$$

was evaluated once at a temperature in the vicinity of  $-8^{\circ}\text{C}$  from the following relations:

$$\lambda = 2.519 \times 10^{-10} \text{ erg/g}$$

$$[k_{f,h}]_{-8^{\circ}\text{C}} = 2422 \text{ erg/cm sec } ^{\circ}\text{C}$$

$$[k_{f,m}]_{N.P., -8^{\circ}\text{C}} = 1.746 \times 10^{-10} \text{ g cm}^2/\text{erg sec}$$

The result was  $(543.5 \times 10^{-6})^{-1}$ , so that, finally,

$$X^{-1} = 543.5 \times 10^{-6} P_{e,l,r} \frac{Nu_h}{Nu_m}$$

Constants  $C_1$ ,  $C_2$ , and  $C_3$  are now defined by the relation

$$P_{d,s} = C_1 + C_2 t_{d,s} + C_3 t_{d,s}^2 \quad (3)$$

where the constants have been given previously in the quadratic expressions (eq. (2)) for vapor pressure. Equation (3) and the psychrometric equation (eq. (1)) are then used to obtain

$$t_{d,s}^2 + \frac{1 + X C_2}{X C_3} t_{d,s} + \frac{C_1 - P_{d,e,l}}{C_3} - \frac{t_{d,e,l}}{X C_3} = 0$$

which may also be written

$$t_{d,s}^2 + a_1 t_{d,s} + a_0 = 0$$

In the latter relation

$$a_1 = C_3^{-1} (X^{-1} + C_2)$$

and

$$a_0 = C_3^{-1} (C_1 - P_{d,e,l} - t_{d,e,l} X^{-1})$$

(The choice as to the particular set of constants to be used is made on the basis of a guess as to the final value of  $t_{d,s}$  itself in borderline cases.)

The droplet temperature is then given by the relation

$$t_{d,s} = -\frac{a_1}{2} + \left(\frac{a_1^2}{4} - a_0\right)^{1/2}$$

The rate of loss of mass is obtained from the expression

$$Q_m = mA_d = h_m A_d (p_{d,s} - p_{d,e,l})$$

in which  $m$  is the mass-loss rate in  $\text{g/cm}^2 \text{ sec}$ , while  $A_d$  is the surface area. Now,

$$h_m = \frac{k_{f,m} \text{Nu}_m}{2r_d}$$

and

$$k_{f,m} \approx (k_{f,m})_{\text{N.P.T.}} \frac{1,013,250}{P_{e,l,r}} \left(\frac{T_{d,e,r}}{273.2}\right)^{0.89}$$

From these,

$$Q_m = 2\pi r_d (p_{d,s} - p_{d,e,l}) \frac{(k_{f,m})_{\text{N.T.P.}} (1,013,250) \text{Nu}_m}{P_{e,l,r}} \left(\frac{T_{d,e,r}}{273.2}\right) \left(\frac{265.2}{273.2}\right)^{-0.11}$$

is obtained; a factor  $(T_{d,e,r}/273.2)^{-0.11}$  has here been replaced by  $(265.2/273.2)^{-0.11}$  to facilitate calculations. The procedure is admissible because of the negligible variation of the factor over the temperature range of interest. The numerical constant then equals

$$2\pi \times 1.746 \times 10^{-10} (0.9707)^{-0.11} \times \frac{1,013,250}{273.2} = 4.082 \times 10^{-6}$$

and the following expression yields the desired mass-loss rate:

$$Q_m = \frac{4.082 \times 10^{-6} r_d T_{d,e,r} (p_{d,s} - p_{d,e,l}) \text{Nu}_m}{P_{e,l,r}}$$

The time rate of loss of fractional mass is then given by

$$\dot{\Lambda} = \frac{3Q_m}{4\pi\rho dr_d^3}$$

The distance rate of loss of fractional mass may be calculated in an elementary manner only if the droplet speed is always positive with respect to the air, and the droplet trajectory and an air streamline virtually coincide. If these conditions are met, the rate  $\Omega$  is given by

$$\Omega = \dot{\Lambda}/(U_L + V_T)$$

In tabulations and graphs  $\Omega$ , which as calculated has the dimensions  $\text{cm}^{-1}$ , appears as the fractional mass lost per foot of droplet travel toward the obstacle.

## RESULTS AND DISCUSSION

The calculations were made for a number of combinations of ambient relative humidity (unity and 0.9), flight altitude (3, 6, 10, 15, 22.5, and 30 thousand ft), ambient temperature (-30, -25, -20, -15, -10, and -5° C), droplet diameter (5, 10, 15, 25, 50, and 150 microns), flight Mach number (0.25, 0.50, 0.75, and 1.0), air-obstacle relative Mach number (0, 0.125, 0.25, 0.50, and 0.75), and droplet-air relative Mach number (0, 0.063, 0.125, 0.25, 0.50, and 0.75). Not all of the possible combinations were used, however, since the number of such combinations is prohibitively large.

The combinations for which calculations were actually made are indicated in the table (table II) in which the results are also presented. The air-obstacle and air-droplet results are not tabulated because they are contained in their entireties in the flight Mach number results collocation (table II(a) and II(b)). Table III contains a summary of certain entry data (air pressures at various altitudes and temperatures) used in the calculations. Most of the results, with the chief exception of the entire 90 percent humidity group, are also presented in graphic form in figures 2 to 9.

Figure 2 exhibits the fractional mass lost per foot of droplet travel (along a stagnation line) as a function of flight Mach number  $M_\infty$  at a succession of fixed droplet-air relative Mach numbers  $M_{r_1}$  for several local air-obstacle Mach numbers  $M_R$  under ambient conditions as indicated (altitude 10,000 ft, air temperature, -25° C), the droplet diameter remaining at 15 microns. It will be noted that the evaporation



rates increase sharply with increasing  $M_\infty$ , particularly at the higher air-obstacle relative Mach numbers. For example, at an  $M_R$  of 0 and an  $M_R$  of 0.125,  $\Omega$  changes from 0.0047 per foot at an  $M_\infty$  of 0.25 to 0.061 per foot (a factor of 13) at an  $M_\infty$  of 0.75; at an  $M_R$  of 0.50 and an  $M_R$  of 0.125,  $\Omega$  changes from 0.00014 per foot at an  $M_\infty$  of 0.5 to 0.0051 (a factor of 36) at an  $M_\infty$  of 0.75.

This relatively large increase of evaporation rates (on a unit distance basis) is the result of combined action of at least two effects. First, at the lower  $M_R$  values (that is, at nearly full stagnation), the time rate of evaporation will tend to be high irrespective of the  $M_\infty$  value, although it will, of course, increase fairly rapidly with increase of the latter. Second, the increase of droplet speed (with respect to the obstacle) at increasing  $M_\infty$  tends to offset the increase of time rate of evaporation insofar as the fractional loss per unit distance is concerned. The net result is a moderate rate of increase of fractional loss per unit distance with increasing  $M_\infty$  at lower  $M_R$  values. At higher  $M_R$  values (greater than, say, 0.5), however, the time rates of evaporation at  $M_\infty$  values such that the  $M_R$  values in question involve only relatively slight stagnation will be very small. Relatively small increases of  $M_\infty$ , therefore, will markedly increase what may be called the fractions of full stagnation, and there will be a substantial increase of time rates of evaporation under those circumstances. Because the (subsonic)  $M_\infty$  is already moderate or high (greater than about 0.6), the increase in droplet speed with increase of  $M_\infty$  will then play a relatively unimportant role in determining the overall fractional loss-rate characteristic (on a unit distance basis). The reasons for this particular characteristic have been presented in some detail because very similar considerations apply in the cases of trends appearing in the remaining tabulated entries and figures.

Additional results of the same kind are presented in table II(b) for an air temperature of  $-15^\circ\text{C}$ ; the remaining variables have the same values as in the case of the data of figure 2 (tabulated in table II(a)). A detailed comparison between the two sets of results indicates that, as expected, the increases of fractional mass loss per unit distance which occur as a result of the increases of  $M_\infty$  and  $M_T$  and decreases of  $M_R$  are somewhat, although not substantially, more marked at the lower ambient temperature than at the higher. In other respects, the results are similar in the two cases.

For example, at an  $M_R$  of 0 and an  $M_R$  of 0.125 for the  $-15^\circ\text{C}$  air-temperature case,  $\Omega$  changes from 0.0079 at an  $M_\infty$  of 0.25 to 0.090 (a factor of 11) at an  $M_\infty$  of 0.75; at an  $M_R$  of 0.50 and an  $M_R$  of 0.125,  $\Omega$  changes from 0.00024 at an  $M_\infty$  of 0.50 to 0.0081 (a factor of 34) at an  $M_\infty$  of 0.75.

Figures 3 and 4 exhibit mass-loss rates as functions of  $M_R$  and  $M_T$ , respectively, for various sets of conditions. The data are not tabulated in the sequence in which they are plotted in these figures, but are included in the listings of table II(a). The curves of figures 2, 3, and 4, therefore, actually present the same data in different ways. The various curves may be considered to be lines of intersection of planes with warped surfaces of three-dimensional figures. For example, if a surface is formed of all points for which  $M = 0.50$ , the vertical axis representing  $\Omega$  and the other axes  $M_R$  and  $M_T$ , then the curves of figures 3(a) and 4(a) are lines of intersection of vertical planes parallel to the  $M_R$  and  $M_T$  axes, respectively.

Interpretations of curve trends in the case of the figures 3 and 4 are difficult; it may, however, be pointed out that, irrespective of time rate of loss of mass, the fractional mass-loss rates (on a unit distance basis) will tend toward infinity whenever both local air speed and relative air-droplet speed tend toward zero. For example, at  $M_R$  values less than 0.10, the fractional mass losses per foot of droplet travel exhibited in figure 3 become of the order of 0.1 as  $M_T$  decreases below 0.125. Physically, this reflects the near absence of motion of the droplet. In the limit, at  $M_R = M_T = 0$ , all droplets will of course evaporate completely.

Droplet size effects are shown in figure 5; the same results are listed in table II(c). It will be noted that while the fractional mass-loss rates decrease, over the droplet size range 5 to 150 microns, by a factor varying between 100 and 10,000, the rates of loss of actual mass increase, over the same droplet size range, by a factor of 270 to 2.7 (in the same order in which the fractional loss rates are given).

Temperature effects are shown in figure 6. These data and a few additional data are tabulated in table II(d). Despite the large changes in vapor pressure in going from an ambient temperature of  $-30^\circ\text{C}$  to one of  $-5^\circ\text{C}$ , the factor of increase in fractional mass lost per foot varies between about 2 and 4 at all combinations of air-obstacle relative Mach number. At other altitudes, flight Mach numbers, and droplet sizes, this factor of increase with temperature remains substantially fixed.

The droplet temperature increase (as is confirmed by values tabulated in this report) is usually about two thirds of the ambient temperature change; hence, the ambient vapor-pressure increase tends to compensate for the liquid-surface vapor-pressure increase.

Altitude effects are shown in figure 7 and are exhibited in numerical form in table II(e). A remarkably small role is played by altitude in the determination of loss rates.

For example, at  $M_\infty = 0.75$ ,  $M_T = 0$ ,  $t_{st,\infty} = -25^\circ \text{C}$ , and  $D = 15$  microns, the increase in going from 3000 to 30,000 feet is about 30 percent; at  $M_\infty = 0.75$ ,  $M_T = 0.25$ , and for the same air temperature and droplet diameter, the increase is about 80 percent. Under certain conditions, this change decreases and even reverses slightly. However, an increase of around 10 percent is typical at the higher evaporation rates. Mutually compensating effects are the lower relative Reynolds numbers (at the lower densities) on one hand and the higher mass-transfer rates (at the lower pressures) on the other.

A few of the calculations (table II(f)) were made on the basis of a free-stream relative humidity of 90 percent, and the balance on the basis of a relative humidity of 100 percent. The droplet equilibrium temperatures in the latter (100 percent) case are between  $0.2^\circ$  and  $0.5^\circ \text{C}$  higher than in the former, while the evaporation rates are slightly lower, the difference usually being of the order of 2 to 7 percent.

The results of calculations for two cases of losses from droplets impinging on cylinders are given in figures 8 and 9. The droplet motions were computed by a numerical technique; the x-motion equation alone of reference 3 was used, since lateral motion was assumed negligible. The air-flow history calculation was based on the assumption that the local velocity was that of incompressible potential flow, although, thereafter, compressible flow relations were used to determine the local air-obstacle relative Mach number  $M_T$ , temperature, pressure, and density. When the x-motion equation was used, account was taken of the changing air density in the local relative Reynolds number. The local evaporation rate was obtained, for each step of the droplet motion, from the curves of figure 3 or 4 by interpolation, the successive products of evaporation rate (on a unit distance basis) and step distance being then summed to obtain total mass losses to the respective points.

It will be noted that the total loss in the case of the 10-centimeter (diameter) cylinder is less than 0.25 percent, while the total loss in the case of the larger (100-centimeter) cylinder is less than 5 percent (the end value was obtainable only by the somewhat uncertain extrapolation indicated by the dashed area of fig. 9). In both cases, most of the evaporation occurs within a distance of one cylinder radius from the cylinder surface.

Finally, it is evident that dynamic calculations would yield very small losses. The internal time constant of a 15-micron liquid water sphere is 0.000023 second (fig. 10). The ratio of approach period to internal time constant  $\Gamma_1$  is 92 for the large cylinder and 9.2 for the smaller. It follows that, in both cases, the internal temperature remains substantially uniform. On the other hand, the ratio of approach period to external time constant is considerably smaller and varies with the local relative heat-transfer Nusselt number. At a distance of 2 radii

from the small cylinder or of about 5 radii from the large cylinder, the Nusselt number is not significantly greater than 2, and the ratio of external to internal time constant is 142, from relation (B6). At those respective distances, therefore, the ratios of approach period to external time constant are  $9.2/142$  or 0.065 for the small cylinder and  $92/142$  or 0.65 for the large one. At points much closer to the cylinder, for example, at a distance of 0.1 radius from either surface, the ratios are about  $9.2/51$  or 0.18 for the small cylinder and  $92/94$  or 1.0 for the large cylinder; the latter figures are based on relative Reynolds numbers of 80 and 10.8, respectively.

It is clear that dynamic thermal response calculations based on external time constant alone (that is, calculations for which internal temperatures were considered uniform) would be valid for 15-micron droplet impingement on either of these cylinders. It is not necessary to make such calculations, however, to draw the qualitative conclusion that the actual total evaporation would be a few percent less than that given previously in the case of the larger cylinder, while the actual loss, in the case of the smaller one, would be considerably smaller than the value determined.

It is clear that total evaporative losses from droplets approaching small or moderately large (up to 100 cm in the transverse direction) obstacles will be of the order of several percent at most for most droplets. If, however, the droplet motional history, irrespective of evaporation, is such that the droplet remains for a very long (or possibly infinitely long) period at a finite distance from the surface, it will, of course, evaporate completely. Discussion of the parameters which determine, in particular cases, the highest droplet diameters for which this will occur is, however, beyond the scope of the present investigation; such diameters, for all but the largest obstacles, will be very small (of the order of 5 microns).

Duct results (quantitatively correct, to a first approximation) may be obtained directly from figures 2, 3, and 4 for a droplet diameter of 15 microns, an altitude of 10,000 feet, and an ambient temperature of  $-25^{\circ}\text{C}$ . Selection of the proper flight Mach number and stagnation  $M_R$  curve for the condition  $M_R = 0$  will yield the desired fractional mass loss rate on a unit distance basis. Selection of the  $M_R = 0$  curves is based on the observation that most of the duct air flow occurs at a constant ram recovery (that is,  $M_R$  value) and that, for a reasonably long duct and small droplet size, the droplet will be essentially at rest with respect to the air over most of the intra-duct droplet history. Further, the internal and external time constants are sufficiently small in comparison with the time spent by the droplet within a duct having a length of at least several feet that quasi-static calculations are not seriously in error.

2734

CJ-3 back

No droplet evaporation will occur when the duct inlet velocity ratio is unity. At the other extreme, let it be assumed that the flight Mach number is 0.75 and the air-duct relative Mach number for intra-duct air is 0.25. At a droplet-air relative Mach number of 0, a value of  $\Omega$  of 0.010 per foot is obtained from table II(a) or figure 2(b) for a droplet of 15-micron diameter at 10,000-foot altitude and  $-25^{\circ}\text{C}$  ambient temperature. Accordingly, the loss for a 10-foot duct would be 10 percent; at a flight Mach number of unity (other conditions remaining the same) the loss would be about 25 percent. . Actually, the loss would be greater in the latter case, since account has not been taken in the present calculation of the increase of fractional mass loss rate with decrease of droplet size. It is possible to conclude that the normal range of droplet mass losses in ducts several feet in length is 0 to 50 percent.

The additional results listed in table II(b) may also, of course, be used for duct or obstacle calculations.

Factors which may be used to correct evaporation rates obtained from figures 2, 3, and 4 (or the data of table II(b)) for departure of droplet diameter, ambient temperature, or altitude from the standard values (15 microns,  $-25^{\circ}\text{C}$ , and 10,000 ft) assumed here may be obtained from figures 5, 6, and 7 or tables II(c), II(d), and II(e). In each case, the procedure required to obtain a correction factor consists merely of noting the ratio of evaporation loss at the nonstandard condition to that at the standard. For example, let the fraction of mass lost per foot of travel of a 10-micron droplet be required for the following conditions:  $M_{\infty}$ , 0.75;  $M_R$ , 0.50;  $M_r$ , 0.25; ambient temperature,  $-10^{\circ}\text{C}$ ; altitude, 30,000 feet. From table II(b) the information is obtained that, at 15 microns,  $-15^{\circ}\text{C}$ , and 30,000 feet, the mass loss rate is 0.0100 per foot. From table II(c) it can be determined that the ratio of loss rate at 10 microns to that at 15 microns for the given values of  $M_{\infty}$ ,  $M_R$ , and  $M_r$  is  $19.4/10.0 = 1.94$ . Table II(d) yields the information that the ratio of loss rate at  $-10^{\circ}\text{C}$  to that at  $-15^{\circ}\text{C}$  is  $12.2/10.0 = 1.22$ . Finally, table II(e) yields the information that the ratio of loss rate at 30,000 feet to that at 10,000 feet is  $7.57/6.25 = 1.21$ . The product of the three factors is 2.87. The mass-loss rate required is therefore  $0.010 \times 2.87 = 0.0287$  per foot. The procedure is not rigorously valid, but the inaccuracies involved are no larger than the inaccuracies inherent in the basic calculations.

## CONCLUSIONS

On the basis of a theoretical analysis of rates of loss by evaporation of atmospheric droplets moving along stagnation lines toward obstacles (such as wings and icing-rate measurement cylinders), it may be concluded that:

1. Little or no evaporative loss occurs from droplets approaching liquid-water-content measurement cylinders (that is, cylinders having diameters less than about 15 cm).

2. Evaporative losses may be as high as several percent in the case of small droplets approaching larger obstacles, such as wings, except that there is always a possibility that the droplet will never reach the airfoil. (In the latter case, it will, of course, evaporate completely if it has been approaching along the stagnation line).

3. Total losses from droplets moving along intake ducts, for example, between the inlet entrance and engine screen of a jet engine, will usually be of the order of 5 to 10 percent at low temperatures for the smaller droplets and a fraction of that for the larger droplets, but may be as great as 50 percent for the smaller droplets at ambient temperatures closer to 0° C for high degrees of stagnation and moderately long (10 ft) ducts.

Lewis Flight Propulsion Laboratory  
National Advisory Committee for Aeronautics  
Cleveland, Ohio, August 17, 1953

## APPENDIX A

## SYMBOLS

The following symbols are used in this report:

$A_d$	droplet surface area, $\text{cm}^2$
$a_0$	$C_3^{-1} (C_1 - p_{d,e,l} - t_{d,e,l} X^{-1}), \text{ } ^\circ\text{C}^2$
$a_1$	$C_3^{-1} (X^{-1} + C_2), \text{ } ^\circ\text{C}$
$C_1, C_2, C_3$	constants of approximate quadratic vapor-pressure equations:
	(a) (b)
	$C_1 = 6136 \text{ or } 5288 \text{ dyne cm}^{-2}$
	$C_2 = 438.7 \text{ or } 287.7 \text{ dyne cm}^{-2} \text{ } ^\circ\text{C}^{-1}$
	$C_3 = 10.69 \text{ or } 4.3047 \text{ dyne cm}^{-2} \text{ } ^\circ\text{C}^{-2}$
$c_{p,d}$	specific heat at constant pressure of liquid water (droplet), $\text{cal g}^{-1} \text{ } ^\circ\text{C}^{-1}$
$D$	diameter, $\text{cm}$
$D_d$	droplet diameter, $\text{cm}$
$G_a$	air mass-flow rate, $\text{g cm}^{-2} \text{ sec}^{-1}$
$h_h$	heat-transfer coefficient, $\text{erg cm}^{-2} \text{ sec}^{-1} \text{ } ^\circ\text{C}^{-1}$
$h_m$	mass-transfer coefficient, $\text{g cm}^{-2} \text{ sec}^{-1} (\text{dyne cm}^{-2})^{-1}$
$j_m$	Colburn mass-transfer parameter defined by relation $j_m \equiv St_m Sc^{2/3}$
$k_{f,h}$	thermal conductivity of material characteristic of film, $\text{erg cm}^{-1} \text{ } ^\circ\text{C}^{-1} \text{ sec}^{-1}$
$k_{f,m}$	mass-transfer conductivity of material characteristic of film and of diffusing material, $\frac{\rho_a \beta}{P_a} \left( \frac{M_d}{M_a} \right), \text{ g cm}^{-2} \text{ sec}^{-1}$ $(\text{dyne cm}^{-3})^{-1}$
$k_{h,a}$	thermal conductivity of air, $\text{erg cm}^{-1} \text{ } ^\circ\text{C}^{-1} \text{ sec}^{-1}$

$k_{h,d}$	thermal conductivity of droplet, $\text{erg cm}^{-1} \text{ } ^\circ\text{C}^{-1} \text{ sec}^{-1}$
$M_a$	molecular weight of dry air, $\text{g (22.4} \times 10^3 \text{ cm}^3)^{-1}$
$M_d$	molecular weight of water, $\text{g (22.4} \times 10^3 \text{ cm}^3)^{-1}$
$M_R$	local Mach number of air flow with respect to obstacle
$M_r$	local relative air-droplet Mach number
$M_\infty$	flight Mach number
$m$	(1) constant equal to 1, 2, or 3 as discussed in text in appendix B (2) mass-transfer rate, $\text{g sec}^{-1} \text{ cm}^{-2}$
$N.P.$	normal pressure (1 atm), $1,013,250 \text{ dyne cm}^{-2}$
$Nu_h$	Nusselt number for heat transfer, $h_h D / k_{f,h}$
$Nu_m$	Nusselt number for mass transfer, $h_m D_d / k_{f,m}$
$P$	air pressure, $\text{dyne cm}^{-2}$
$P_a$	mean local dry-air partial pressure, $\text{dyne cm}^{-2}$
$P_{e,l,r}$	local effective relative air pressure, $\text{dyne cm}^{-2}$
$P_{st,\infty}$	static ambient flight air pressure (at infinity), $\text{dyne cm}^{-2}$
$Pr$	Prandtl number
$p_{d,s}$	droplet equilibrium (psychrometric) vapor pressure, $\text{dyne cm}^{-2}$
$p_{d,\infty}$	ambient static flight water vapor pressure (at infinity), $\text{dyne cm}^{-2}$
$p_{d,e,l}$	local effective water vapor pressure, $\text{dyne cm}^{-2}$
$Q_m$	rate of loss of mass of droplet, $\text{g sec}^{-1}$
$R$	principal (ref.) dimension of obstacle, cm
$Re$	Reynolds number



$Re_r$	relative air-droplet Reynolds number based upon local static air density, droplet diameter, relative air-droplet air speed, and viscosity at the relative air-droplet total temperature
$r_d$	droplet radius, cm
$Sc$	Schmidt number, $\mu_a/\rho_a\beta$
$St_m$	Stanton number for mass transfer
$T$	absolute temperature, $^{\circ}K$
$\overline{T_d}$	volume-mean droplet temperature, $^{\circ}K$
$T_{d,e,l}$	effective local air temperature with respect to droplet, $^{\circ}K$
$T_{d,t,l}$	air total temperature with respect to droplet, $^{\circ}K$
$T_{st,l}$	local static air temperature, $^{\circ}K$
$T_{st,\infty}$	ambient (flight) static air temperature, $^{\circ}K$
$T_t$	air total temperature with respect to obstacle, $^{\circ}K$
$t$	temperature, $^{\circ}C$
$t_{d,e,l}$	effective local air temperature with respect to droplet, $^{\circ}C$
$t_{d,s}$	equilibrium (psychrometric) droplet temperature, $^{\circ}C$
$t_{st,\infty}$	ambient (flight) static air temperature, $^{\circ}C$
$U_l$	local air speed with respect to obstacle, $cm\ sec^{-1}$
$U_{\infty}$	flight obstacle speed, $cm\ sec^{-1}$
$V_r$	local air-droplet relative speed, $cm\ sec^{-1}$
$X$	$\lambda h_m/h_h$ , $^{\circ}C\ (dyne\ cm^{-2})^{-1}$
$\beta$	diffusion coefficient, $cm^2\ sec^{-1}$
$\beta_0$	diffusion coefficient at $0^{\circ}C$ and atmospheric pressure, $cm^2\ sec^{-1}$

$\Gamma_i$	number of internal sphere time constants per unit of time required for obstacle to move through air at speed $U_\infty$ a distance $R$
$\gamma$	ratio of specific heats
$\theta$	time, sec
$\theta_{d,ext}$	external time constant of object (sphere), sec
$\theta_{d,int}$	internal time constant of object (sphere), sec
$\kappa_d$	thermal diffusivity of droplet (water), $\text{cm}^2 \text{sec}^{-1}$
$\Lambda$	time rate of loss of fractional mass, $\text{sec}^{-1}$
$\lambda$	heat of vaporization, $\text{erg g}^{-1}$
$\mu$	viscosity of air, poise
$\mu_t$	viscosity of air at temperature $T_{d,t,l}$ , poise
$\rho$	density, $\text{g cm}^{-3}$
$\rho_d$	droplet (water) density, $\text{g cm}^{-3}$
$\rho_{st,l}$	local static air density, $\text{g cm}^{-3}$
$\sigma$	flight relative humidity
$\Omega$	fractional droplet mass lost per centimeter of droplet travel toward obstacle; loss per foot is given in tabulations and graphs

Subscripts:

a	appertaining to air
d	appertaining to droplet
e	effective value
f	appertaining to film
h	heat transfer
l	local

2734

63-4

m	mass transfer
N.P.	normal (atmospheric) pressure
N.T.P.	normal (atmospheric) pressure and (0° C) temperature
R	air-obstacle relative value
r	droplet-air relative value
s	equilibrium (psychrometric) value
st	static value
t	total value
$\infty$	value in undisturbed stream

## APPENDIX B

## SPHERE TIME CONSTANTS

The thermal response of a solid body may, to a first approximation, be described in terms of what may be designated an "internal time constant" and an "external time constant." (Although liquid spheres are discussed in this report, they are treated as though solid.) For present purposes the internal time constant is designated  $\theta_{d,int}$  and is defined as the time required for the mean sphere temperature to change by  $1-e^{-1}$  of the asymptotic change upon imposition of an instantaneous surface temperature change. The external time constant is designated  $\theta_{d,ext}$  and is defined as the time required for the sphere temperature (assumed uniform throughout) to change by  $1-e^{-1}$  of the asymptotic change upon imposition of an instantaneous environmental temperature change.

From curve V, figure 9, page 84 of reference 15, it is found that the Fourier modulus  $\kappa_d \theta / r_d^2$  has, in the case of the sphere, the value 0.056 when the temperature ratio  $\bar{T}_d / T_s = 0.632$ ; consequently, the internal time constant of a sphere is given approximately by the relation

$$\theta_{d,int} = 0.056 r_d^2 / \kappa_d \quad (B1)$$

In the case of water,  $\kappa_d = 0.00136$  at  $0^\circ \text{C}$ , in c.g.s.-calorie units, and it is found that  $\theta_{d,int} = 41 \cdot r_d^2$ ;  $r_d$  is here given in centimeters. Figure 10 exhibits this relation over the range  $D_d = 2r_d = 1$  to 1000 microns, over which  $\theta_{d,int}$  varies between  $\sim 10^{-7}$  and  $10^{-1}$  second. At a typical droplet size, 10 microns, the time constant is about  $10^{-5}$  second.

The question arises as to the magnitude of this period as compared with the approach time of a droplet.

If  $\Gamma_1$  is defined as the number of internal sphere time constants per unit of time required for the air (or droplet) at infinity to move (relatively) through a distance equal to the selected principal dimension of the obstacle, the relation

$$\Gamma_1 = \frac{R}{41 \cdot r_d^2 U_\infty} \quad (B2)$$

2734

CJ-4 back

applies (the cylinder radius has been selected as the principal dimension, rather than the diameter).

Values of  $\Gamma_1$  are plotted in figure 11 as a function of  $U_\infty$  for a number of combinations of  $R$  and  $D_d$ . The range of  $\Gamma_1$  covered is about 0.01 to 1000, of  $U_\infty$  225 to 825 miles per hour, of  $R$  0.5 to 180 centimeters, and of  $D_d$  6.25 to 400 microns. It is clear that for large ( $>5$ , say) values of  $\Gamma_1$  the sphere temperature will be uniform except possibly in regions of maximum rate of air temperature change, where small gradients will exist. On the other hand, it may be stated without proof that for small ( $<0.2$ ) values, it is possible to make an estimate of the fractional volume (adjacent to the surface) of the sphere which alone participates, to a first approximation, in the thermal exchanges with the environment, and so to make rough calculations using, in effect, a hollow sphere in the liquid portion of which the temperature is taken to be uniform. In the region  $0.2 < \Gamma_1 < 5$ , roughly, no simple approach appears to be possible; this region is accordingly labeled "critical region" in figure 2.

It will be noted that many combinations of liquid-water-content measuring cylinder diameter and droplet diameter fall within or near the critical region. While it is possible to deduce that in such cases the droplet surface temperatures will be higher than they will be for first-order response (that is, the response of the sphere as a unit), it is not easy to make quantitative evaluations.

In the subcritical region the (approximate) calculations based on the "shell" concept, while possibly easier, will lead to results varying very widely with the particular conditions, and such calculations are accordingly not made in the present report. Again, in general, surface temperatures will be higher, and usually markedly so, than those attained on the basis of first-order response.

The external time constant  $\theta_{d,ext}$  in the case of heat transfer without evaporation appears, for example, as a by-product of investigations of heat transfer to and from solid bodies through uniform boundary layers as carried out by several investigators. Jakob (ref. 16, pp. 270-291) summarizes their results and, in particular, presents (p. 291) a chart in which exponential changes of (uniform) plate, cylinder and sphere temperatures are given as functions of the variable  $\frac{m k_d h_h \theta}{k_{h,d} r_d}$ . In that expression,  $m$  has the values 1, 2, and 3 for plate, cylinder, and sphere, respectively, and  $r_d$  is half the plate thickness or, otherwise, the body radius. When the variable in question equals unity,  $\theta$  equals  $\theta_{d,ext}$  by definition and, in the case of the sphere, the relation

$$\theta_{d,ext} = \frac{k_{h,d} r_d}{3k_d h_h} = \frac{\rho_d c_{p,d} r_d}{3h_h} \quad (B3)$$

is obtained. The same relation is, of course, obtainable very directly and simply by considering that the system sphere-boundary layer behaves like an electrical resistance-capacity circuit of capacity  $(4\pi/3)r_d^3 \rho_d c_{p,d}$  and resistance  $\frac{1}{4\pi r_d^2 h_h}$ , the product  $RC$  then yielding  $\theta_{d,ext}$ . For many purposes it is preferable to use the Nusselt number of heat transfer

$$Nu_h = \frac{h_h D_d}{k_{h,a}}$$

when  $Nu_h$  is used, this equation becomes

$$\theta_{d,ext} = \frac{2r_d^2 \rho_d c_{p,d}}{3k_{h,a} Nu_h} \quad (B4)$$

It is known that

$$Nu_h \propto Re_r^{0.6}$$

and it is instructive to note, therefore, that

$$\theta_{d,ext} \propto \frac{D_d^{1.4} \rho_d c_{p,d}}{k_{h,a}}$$

(Obviously, air relative speed, air density, and air viscosity factors have been omitted.)

In view of the fact that, in contra-distinction to  $\theta_{d,int}$ ,  $\theta_{d,ext}$  depends on a comparatively large number of factors, it did not appear worthwhile to present any set of curves from which its magnitude might be estimated. On the other hand, a direct comparison with  $\theta_{d,int}$  is fruitful. It is clear that

$$\frac{\theta_{d,ext}}{\theta_{d,int}} = \frac{11.9 k_{h,d}}{k_{h,a} Nu_h} \quad (B5)$$

Upon evaluation of the thermal conductivities of air and liquid water at 0° C, it is found that

$$\frac{\theta_{d,ext}}{\theta_{d,int}} = \frac{284}{Nu_h} \quad (B6)$$

in the case of a sphere of liquid water in air at 0° C.

It is generally accepted, on the basis of both theory and observation (ref. 11, for example), that the minimum value of  $Nu_h$  is 2. The maximum value that the relative Reynolds number of a droplet-air system is likely to reach, for flight Mach numbers less than unity, is about 1000, at which Reynolds number the value of  $Nu_h$  (ref. 11, fig. 9) will be about 20. The range of the ratio of equation (B6) will therefore be about 10:1, from values of about 140 (extreme high) through typical values of the order of 40 to values of about 14 (extreme low).

When evaporation (or, in general, mass transfer) is occurring, the situation is not so simple since latent heat of vaporization or condensation may be either hastening or slowing down a particular droplet temperature change. It is to be noted that if the environment of a large droplet is suddenly altered by an adiabatic compression, some condensation may conceivably occur before the instant at which the droplet-surface vapor pressure, as a result of surface-temperature rise, once again equals or exceeds the increased ambient water vapor pressure. Initially, then, the addition of heat of condensation to droplet heat content would tend to accelerate surface temperature rise and, therefore, decrease the initial time constant.

In general, then, even the first-order response cannot be calculated unless assumptions are made concerning condensation rates in the case of larger droplets or unless the situation is that of approach of small droplets (5 to 20 microns) to obstacles that are not small.


#### REFERENCES

1. Guibert, A. G., Janssen, E., and Robbins, W. M.: Determination of Rate, Area, and Distribution of Impingement of Waterdrops on Various Airfoils from Trajectories Obtained on the Differential Analyzer. NACA RM 9A05, 1949.
2. Bergrun, Norman R.: A Method for Numerically Calculating the Area and Distribution of Water Impingement on the Leading Edge of an Airfoil in a Cloud. NACA TN 1397, 1947.
3. Langmuir, Irving, and Blodgett, Katherine B.: A Mathematical Investigation of Water Droplet Trajectories. Tech. Rep. No. 5418, Air Materiel Command, AAF, Feb. 19, 1946. (Contract No. W-33-038-ac-9151 with General Electric Co.)
4. Hardy, J. K.: Evaporation of Drops of Liquid. Rep. No. Mech. Eng. 1, British R.A.E., Mar. 1947.
5. Langmuir, Irving: The Cooling of Cylinders by Fog Moving at High Velocities. General Electric Co., Mar. 1945.

2734


- 2734
6. Schmidt, Ernst, and Wenner, Karl: Heat Transfer over the Circumference of a Heated Cylinder in Transverse Flow. NACA TM 1050, 1943.
  7. Frössling, Nils: Über die Verdunstung Fallender Tropfen. Gerl. Beitr. Geophys., Bd. 52, Heft 1/2, 1938, pp. 170-216.
  8. Homann, F. (D. C. Ipsen, trans.): The Effect of High Viscosity on the Flow Around a Cylinder and Around a Sphere. Rep. No. HE-150-88, Inst. Eng. Res., Univ. Calif., Berkeley (Calif.), July 17, 1951. (Contract NAW-6004.)
  9. Kaplan, Carl: The Flow of a Compressible Fluid Past a Sphere. NACA TN 762, 1940.
  10. Goff, John A., and Gratch, Serge: The Saturation Pressure of Water below 60° C. Rep. No. 4546, Thermodynamics Research Lab., Univ. of Pennsylvania, Jan. 1948. (Navy contract NObs-2477.)
  11. Williams, Glenn Carber: Heat Transfer, Mass Transfer and Friction for Spheres. SC. D. Thesis, M.I.T., 1942.
  12. Ingebo, Robert D.: Vaporization Rates and Heat-Transfer Coefficients for Pure Liquid Drops. NACA TN 2368, 1951.
  13. Boelter, L. M. K., Cherry, V. H., Johnson, H. A., and Martinelli, R. C.: Heat Transfer Notes. Univ. Calif. Press (Berkeley and Los Angeles), 1948.
  14. Dorsey, N. Ernest: Properties of Ordinary Water-Substance. Reinhold Pub. Corp. (New York), 1940.
  15. Carslaw, H. S., and Jaeger, J. C.: Conduction of Heat in Solids. Clarendon Press (Oxford), 1947.
  16. Jakob, Max: Heat Transfer. Vol. I. John Wiley & Sons, Inc., 1949.



TABLE I. - COMPARISON OF ACTUAL VAPOR PRESSURES AND PRESSURES  
GIVEN BY EQUATIONS (2a) AND (2b)


Temperature, °C	Actual vapor pressure, dyne cm <sup>-2</sup>	Pressure (eq. (2a))	Error, percent (eq. (2a))	Pressure (eq. (2b))	Error, percent (eq. (2b))
-32.0	421			490	+16.4
-31.5	441			497	+12.7
-31.0	463			506	+9.3
-30.5	485			518	+6.8
-30.0	509			531	+4.3
-29.5	533			547	+2.6
-29.0	559			565	+1.1
-28.5	586			585	-.17
-28.0	613			607	-.98
-27.5	643			632	-1.7
-27.0	673			658	-2.2
-26.5	704			687	-2.4
-26.0	737			718	-2.6
-25.5	771			751	-2.6
-25.0	807			786	-2.6
-24.5	844			823	-2.5
-24.0	883			863	-2.3
-23.5	923			905	-2.0
-23.0	965			948	-1.8
-22.5	1008			994	-1.4
-22.0	1054			1042	-1.1
-21.5	1101			1093	-.73
-21.0	1150			1144	-.52
-20.5	1201			1199	-.17
-20.0	1254			1256	+.16
-19.5	1309			1315	+.46
-19.0	1366			1376	+.73
-18.5	1426			1439	+.91
-18.0	1488			1504	+1.1
-17.5	1552	1733	+11.7	1572	+1.3
-17.0	1619	1768	+9.2	1641	+1.4

TABLE I. - Continued. COMPARISON OF ACTUAL VAPOR PRESSURES AND PRESSURES GIVEN BY EQUATIONS (2a) AND (2b)



Temperature, °C	Actual vapor pressure, dyne cm <sup>-2</sup>	Pressure (eq. (2a))	Error, percent (eq. (2a))	Pressure (eq. (2b))	Error, percent (eq. (2b))
-16.5	1688	1808	+7.1	1713	+1.5
-16.0	1760	1853	+5.3	1787	+1.5
-15.5	1834	1905	+3.9	1863	+1.6
-15.0	1912	1961	+2.6	1941	+1.5
-14.5	1992	2023	+1.6	2022	+1.5
-14.0	2076	2089	+.63	2104	+1.3
-13.5	2162	2162	0	2189	+1.2
-13.0	2252	2239	-.50	2275	+1.0
-12.5	2345	2323	-.94	2365	+.85
-12.0	2441	2411	-1.2	2456	+.61
-11.5	2541	2505	-1.4	2549	+.31
-11.0	2644	2604	-1.5	2644	0
-10.5	2752	2709	-1.6	2742	-.36
-10.0	2863	2818	-1.6	2841	-.77
-9.5	2978	2933	-1.5	2943	-1.2
-9.0	3097	3054	-1.4	3048	-1.6
-8.5	3221	3179	-1.3	3154	-2.1
-8.0	3348	3311	-1.1	3262	-2.6
-7.5	3481	3447	-.98	3372	-3.1
-7.0	3618	3589	-.80	3485	-3.7
-6.5	3759	3736	-.61	3600	-4.2
-6.0	3906	3889	-.44	3717	-4.8
-5.5	4058	4047	-.27		
-5.0	4215	4210	-.12		
-4.5	4377	4378	+.12		
-4.0	4545	4552	+.15		
-3.5	4719	4732	+.28		
-3.0	4898	4916	+.37		
-2.5	5084	5106	+.43		
-2.0	5275	5301	+.49		
-1.5	5473	5502	+.53		
-1.0	5678	5708	+.53		

2734

9-10

TABLE I. - Concluded. COMPARISON OF ACTUAL VAPOR PRESSURES AND PRESSURES GIVEN BY EQUATIONS (2a) AND (2b)



Temperature, °C	Actual vapor pressure, dyne cm <sup>-2</sup>	Pressure (eq. (2a))	Error, percent (eq. (2a))	Pressure (eq. (2b))	Error, percent (eq. (2b))
-0.5	5889	5919	+ .50		
0	6108	6136	+ .46		
.5	6333	6358	+ .39		
1.0	6566	6585	+ .29		
1.5	6807	6818	+ .16		
2.0	7055	7056	+ .01		
2.5	7311	7300	- .15		
3.0	7575	7548	- .36		
3.5	7848	7802	- .59		
4.0	8129	8062	- .82		
4.5	8420	8327	-1.1		
5.0	8719	8597	-1.4		
5.5	9028	8872	-1.7		
6.0	9347	9153	-2.1		
6.5	9675	9439	-2.4		
7.0	10013	9731	-2.8		
7.5	10362	10028	-3.2		
8.0	10722	10330	-3.7		
8.5	11092	10637	-4.1		
9.0	11474	10950	-4.6		
9.5	11867	11268	-5.0		
10.0	12272	11592	-5.5		
10.5	12690	11921	-6.1		
11.0	13119	12255	-6.6		
11.5	13562	12595	-7.1		
12.0	14017	12940	-7.7		
12.5	14486	13291	-8.2		
13.0	14969	13646	-8.8		
13.5	15466	14007	-9.4		
14.0	15977	14373	-10.0		
14.5	16503	14745	-10.7		
15.0	17044	15122	-11.3		

TABLE II - RESULTS

(a) Flight Mach number effects at  $-25^{\circ}\text{C}$ .

$D_d$ , microns	Altitude, ft)	$t_{d,0}$ , $^{\circ}\text{C}$	$M_{\infty}$	$M_R$	$M_r$	$V_r$ , ft/sec	$Re_r$	$t_{d,s}$ , $^{\circ}\text{C}$	$Q_m$ , g/sec	$\Delta$ , fractional mass/sec	$U_r + V_r$ , ft/sec	$\Omega$ , fractional mass/ft
15	10,000	-25	0.25	0	0.063	65.68	18.12	-22.29	$0.76 \times 10^{-9}$	0.43	65.68	$6.59 \times 10^{-3}$
			.50			66.86	19.64	-14.94	3.79	2.14	66.86	32.0
			.75			68.85	22.32	-3.86	11.5	6.53	68.85	94.9
			1.00			71.52	26.51	9.66	28.6	16.2	71.52	226
			.25		.125	130.3	35.89	-21.88	1.08	.613	130.3	4.71
			.50			132.7	38.90	-14.52	4.85	2.75	132.7	20.7
			.75			136.6	44.28	-3.44	14.6	8.28	136.6	60.6
			1.00			141.9	52.46	10.14	36.2	20.5	141.9	145
			.25		.25	260.6	71.30	-20.33	2.14	1.21	260.6	4.64
			.50			265.4	77.25	-12.96	7.28	4.12	265.4	15.5
			.75			273.1	87.95	-1.96	20.8	11.8	273.1	43.2
			1.00			283.8	104.3	11.79	50.1	28.3	283.8	99.9
			.50		.50	530.8	150.3	-6.98	$1.62 \times 10^{-8}$	9.18	530.8	17.3
			.75			546.3	171.0	3.69	3.90	22.1	546.3	40.4
			1.00			567.6	202.8	$^{17.89}$	8.29	46.9	567.6	82.6
			.75		.75	819.5	245.9	12.87	7.09	40.1	819.5	48.9
			1.00			851.4	291.8	$^{28.01}$			851.4	
			.50	.25	0	0	0	-17.45	$1.41 \times 10^{-9}$	.798	263.8	3.03
			.75					-5.98	4.98	2.82	271.5	10.4
			1.00					7.78	12.9	7.30	282.0	25.9
			.25		.063	65.26	17.64	-24.88	.027	.012	524.2	.056
			.50			66.50	19.14	-17.42	2.62	1.48	530.4	4.49
			.75			68.40	21.74	-6.11	9.43	5.34	539.9	15.7
			1.00			71.09	25.79	7.44	25.4	14.4	553.2	40.6
			.25		.125	129.5	34.92	-24.46	.16	.088	388.5	.23
			.50			131.9	37.83	-17.03	3.38	1.92	395.7	4.84
			.75			135.8	43.05	-5.71	12.0	6.76	407.3	16.8
			1.00			141.1	51.03	7.90	32.1	18.2	423.1	42.9
			.25		.25	259.0	69.38	-22.89	.84	.47	517.9	.91
			.50			263.9	75.17	-15.47	5.31	3.00	527.7	5.69
			.75			271.5	85.50	-4.21	17.2	9.73	543.0	17.9
			1.00			282.2	101.4	9.52	44.5	25.2	584.3	44.6
			.50		.50	527.9	146.2	-9.38	12.7	7.19	791.7	9.08
			.75			543.0	166.4	1.42	33.3	18.8	814.6	23.1
			1.00			564.3	197.3	$^{15.50}$	74.6	42.2	846.4	49.9
			.75		.75	814.7	239.0	10.52	$6.27 \times 10^{-8}$	35.5	1086	32.7
			1.00			846.5	283.7	$^{25.43}$			1129	
			.75	.50	0	0	0	-13.11	$2.52 \times 10^{-9}$	1.43	533.1	2.68
			1.00					1.19	8.74	4.94	553.8	8.95
			.50		.063	65.26	17.64	-24.88	.027	.016	583.3	.027
			.75			67.16	20.03	-13.13	4.71	2.67	600.3	4.44
			1.00			69.78	23.75	.96	16.8	9.52	623.6	15.3
			.50		.125	129.5	34.92	-24.46	.16	.091	647.5	.14
			.75			133.2	39.69	-12.73	6.00	3.40	666.4	5.10
			1.00			138.5	47.01	1.38	21.3	12.1	692.2	17.4
			.50		.25	259.0	69.38	-22.89	.84	.47	777.2	.61
			.75			266.5	78.85	-11.14	8.83	5.00	799.5	6.25
			1.00			276.9	93.44	2.91	29.9	16.9	830.7	20.4
			.50		.50	518.1	134.8	-16.77	5.22	2.96	1036	2.85
			.75			533.2	153.3	-5.29	19.1	10.8	1066	10.2
			1.00			553.8	181.7	8.66	52.8	29.9	1108	27.0
			.75		.75	799.6	220.2	3.70	$4.18 \times 10^{-8}$	23.6	1333	17.7
			1.00			850.7	261.2	$^{18.09}$	9.01	51.0	1384	36.8
			.75	.75	0	0	0	-9.49	$3.58 \times 10^{-9}$	2.02	807.1	2.51
			.75		.063	65.26	17.64	-24.88	.027	.016	842.2	.018
			1.00			67.78	20.85	-9.57	6.73	3.81	875.0	4.35
			.75		.125	129.5	34.92	-24.47	.16	.088	906.5	.097
			1.00			134.5	41.31	-9.14	8.51	4.82	941.6	5.12
			.75		.25	259.0	69.38	-22.89	.84	.47	1036	.46
			1.00			269.0	82.10	-7.63	12.4	7.03	1076	6.54
			.75		.50	518.1	134.8	-16.77	5.22	2.96	1295	2.28
			1.00			538.1	159.5	-1.97	25.6	14.5	1345	10.8
			.75		.75	776.9	193.4	-7.12	16.9	9.57	1554	6.16
			1.00			807.1	229.2	7.03	51.5	29.2	1614	18.1

<sup>a</sup>Droplet temperatures and evaporation rates not quantitative for calculated droplet temperatures higher than about  $15^{\circ}\text{C}$ .  
Evaporation rates omitted for droplet temperatures greater than  $25^{\circ}\text{C}$ .

2734

CJ-5 back

TABLE II - Continued. RESULTS

(b) Flight Mach number effects at  $-15^{\circ}\text{C}$ .

$D_d$ , microns	Altitude, ft	$t_{d,s}$ , $^{\circ}\text{C}$	$M_{\infty}$	$M_R$	$M_T$	$V_T$ , ft/sec	$Re_T$	$t_{d,s}$ , $^{\circ}\text{C}$	$Q_m$ , g/sec	$\Lambda$ , fractional mass/sec	$U_T + V_T$ , ft/sec	$\Omega$ , fractional mass/ft
15	10,000	-15	0.25	0	0.063	66.96	17.48	-12.52	$1.34 \times 10^{-9}$	0.757	66.96	$11.3 \times 10^{-3}$
			.50			68.24	18.96	-5.86	6.14	3.47	68.24	50.9
			.75			70.18	21.57	3.93	17.6	9.98	70.18	142
			1.00			72.93	25.58	<sup>a</sup> 17.07	38.4	21.7	72.93	298
			.25		.125	132.8	34.62	-12.15	1.85	1.05	132.8	7.89
			.50			135.4	37.58	-5.50	7.86	4.45	135.4	32.9
			.75			139.3	42.75	4.34	22.2	12.6	139.3	90.3
			1.00			144.7	50.70	<sup>a</sup> 17.59	48.5	27.5	144.7	190
			.25		.25	265.7	68.78	-10.68	3.53	2.00	265.7	7.52
			.50			270.8	74.63	-4.11	11.9	6.72	270.8	24.8
			.75			278.5	84.95	5.79	31.1	17.6	278.5	63.2
			1.00			289.4	100.8	<sup>a</sup> 19.30	66.5	37.6	289.4	130
			.50		.50	541.7	145.1	1.21	$2.70 \times 10^{-8}$	15.3	541.7	28.2
			.75			557.1	165.3	11.35	5.51	31.2	557.1	55.9
			1.00			578.7	196.1	<sup>a</sup> 25.54			578.7	
			.75		.75	835.6	237.6	<sup>a</sup> 20.58	9.38	53.1	835.6	63.5
			1.00			868.1	282.2	35.95			868.1	
			.50	.25	0	0	0	-7.96	$2.25 \times 10^{-9}$	1.27	269.0	4.73
			.75					2.05	7.99	4.52	276.9	16.3
			1.00					<sup>a</sup> 15.29	17.8	10.1	287.7	35.1
			.25		.063	66.57	17.01	-14.89	.046	.026	330.8	.078
			.50			67.85	18.45	-7.96	4.11	2.33	337.0	6.90
			.75			69.78	20.99	1.84	14.8	8.39	346.7	24.2
			1.00			72.51	24.90	14.8	34.5	19.5	360.2	54.2
			.25		.125	132.1	33.69	-14.52	.28	.16	396.3	.41
			.50			134.6	36.53	-7.68	5.47	3.10	403.6	7.67
			.75			138.5	41.58	<sup>a</sup> 2.25	18.7	10.6	415.3	25.5
			1.00			143.9	49.29	<sup>a</sup> 15.34	43.6	24.6	431.5	57.1
			.25		.25	264.2	66.93	-13.06	1.46	.827	528.4	1.57
			.50			269.2	72.57	-6.28	8.62	4.88	538.4	9.06
			.75			276.9	82.59	3.66	26.4	14.9	553.8	27.0
			1.00			287.7	97.91	<sup>a</sup> 17.00	59.8	33.8	575.5	58.8
			.50		.50	538.4	141.1	-.96	20.9	11.8	807.7	14.7
			.75			553.8	160.7	9.15	48.1	27.2	830.7	32.8
			1.00			575.5	190.5	<sup>a</sup> 23.12	97.1	54.9	863.2	63.7
			.75		.75	830.7	230.9	<sup>a</sup> 18.23	$8.43 \times 10^{-8}$	47.7	1108	43.0
			1.00			863.2	274.1	33.35			1151	
			.75	.50	0	0	0	-4.24	$4.18 \times 10^{-9}$	2.36	543.6	4.35
			1.00					8.83	12.8	7.24	565.0	12.8
			.50		.063	66.57	17.01	-14.89	.046	.026	595.1	.043
			.75			68.50	19.32	-4.31	7.66	4.34	612.1	7.08
			1.00			71.19	22.92	8.52	24.3	13.7	656.1	21.6
			.50		.125	132.1	33.69	-14.52	.28	.16	660.6	.24
			.75			135.9	38.34	-3.95	9.77	5.53	679.6	8.13
			1.00			141.2	45.42	8.96	30.6	17.3	706.2	24.5
			.50		.25	264.2	66.93	-13.06	1.46	.827	792.8	1.04
			.75			271.8	76.10	-2.55	14.4	8.17	815.6	10.0
			1.00			282.5	90.24	10.47	42.3	24.0	847.4	28.3
			.50		.50	528.6	130.1	-7.36	8.43	4.77	1057	4.52
			.75			543.7	148.0	2.76	30.0	17.0	1087	15.6
			1.00			565.0	175.7	<sup>a</sup> 16.25	71.6	40.5	1130	35.9
			.75		.75	815.7	212.7	11.48	$5.92 \times 10^{-8}$	33.5	1359	24.6
			1.00			847.5	252.6	<sup>a</sup> 25.86			1412	
			1.00	.75	0	0	0	-1.13	$5.96 \times 10^{-9}$	3.37	823.5	4.10
			.75		.063	66.57	17.01	-14.89	.046	.026	859.2	.030
			1.00			69.16	20.15	-1.27	11.0	6.22	892.7	6.97
			.75		.125	132.1	33.69	-14.52	.28	.16	924.9	.17
			1.00			137.2	39.90	-.89	13.9	7.87	960.6	8.19
			.75		.25	264.2	66.90	-13.06	1.46	.827	1057	.783
			1.00			274.5	79.22	.52	20.0	11.3	1098	10.3
			.75		.50	528.6	130.1	-7.36	8.43	4.77	1321	3.61
			1.00			548.9	154.0	5.89	38.4	21.7	1372	15.8
			.75		.75	792.7	186.8	1.20	27.3	15.5	1585	9.75
			1.00			823.5	221.6	14.77	71.0	40.2	1647	24.4

<sup>a</sup>Droplet temperatures and evaporation rates not quantitative for calculated droplet temperatures higher than about  $15^{\circ}\text{C}$ .  
Evaporation rates omitted for droplet temperatures greater than  $25^{\circ}\text{C}$ .

TABLE II - Continued. RESULTS

(c) Droplet diameter effects.



$D_d$ , microns	Altitude, ft	$t_{gt,0}$ , °C	$M_\infty$	$M_R$	$M_T$	$V_T$ , ft/sec	$Re_T$	$t_{d,0}$ , °C	$Q_m$ , g/sec	$A$ , fractional mass/sec	$U_T + V_T$ , ft/sec	$\Omega$ , fractional mass/ft
5	10,000	-15	0.75	0	0.063	70.18	7.190	3.91	$4.57 \times 10^{-9}$	69.8	70.18	$995 \times 10^{-3}$
10							14.38	3.91	10.6	20.2		288
15							21.57	3.93	17.6	9.98		142
25							35.95	3.97	34.2	4.18		59.5
50							71.90	4.09	87.3	1.33		19.0
150							215.7	4.40	418	.236		3.37
5					.25	278.5	28.32	5.58	7.07	108		388
10							56.64	5.70	17.8	34.0		122
15							84.94	5.79	31.1	17.6		65.2
25							141.6	5.94	64.2	7.84		28.2
50							283.2	6.17	176	2.69		9.66
150							849.4	6.61	921	.521		1.87
5					.75	835.6	79.20	20.01	$1.94 \times 10^{-8}$	297		355
10							158.4	20.35	5.20	99.3		119
15							257.6	20.58	9.58	53.1		53.5
25							396.0	20.92	20.1	24.5		29.3
50							792.0	21.39	57.3	8.75		10.5
150							2376	22.22	313	1.77		2.12
5					.25	0	0	2.05	$2.66 \times 10^{-9}$	40.7	276.9	147
10										10.2		36.7
15										4.52		16.3
25										1.83		5.87
50										.407		1.47
150										.045		.163
5					.063	69.78	6.995	1.83	3.86	58.9	346.7	170
10							13.99	1.83	8.92	17.0		49.1
15							20.99	1.84	14.8	8.39		24.2
25							34.98	1.88	28.7	3.51		10.1
50							69.95	1.99	73.2	1.12		3.23
150							209.9	2.24	349	.197		.569
5					.25	276.9	27.53	3.49	6.02	92.0	553.8	166
10							55.06	3.58	15.1	28.9		52.2
15							82.59	3.66	26.4	14.9		27.0
25							137.7	3.79	54.4	6.64		12.0
50							275.3	4.01	149	2.28		4.12
150							825.9	4.39	778	.440		.795
5					.75	830.7	76.95	17.70	$1.75 \times 10^{-8}$	267	3	241
10							153.9	18.00	4.66	89.1		80.4
15							230.9	18.23	8.43	47.7		43.0
25							384.8	18.53	18.0	22.0		19.8
50							769.5	18.97	51.3	7.84		7.08
150							2309	19.46	276	1.56		1.41
5					.50	0	0	-4.24	$1.39 \times 10^{-9}$	21.3	543.6	39.2
10										5.52		9.79
15										4.18		4.35
25										2.56		1.97
50										.851		.392
150										.213		.043
5					.063	68.50	6.440	-4.32	2.01	30.7	612.1	50.1
10							12.88	-4.33	4.61	8.80		14.4
15							19.32	-4.31	7.66	4.34		7.08
25							32.20	-4.30	14.8	1.81		2.95
50							64.40	-4.23	37.4	.572		.934
150							193.2	-4.08	177	.100		.163
5					.25	271.8	25.37	-2.66	$.352 \times 10^{-8}$	50.7	815.6	62.2
10							50.73	-2.61	.828	15.8		19.4
15							76.10	-2.55	1.44	8.17		10.0
25							126.8	-2.48	2.96	3.61		4.43
50							253.7	-2.35	8.06	1.23		1.51
150							761.0	-2.10	41.8	.237		.290
5					.75	815.7	70.90	11.08	1.24	189		139
10							141.8	11.31	3.29	62.8		46.2
15							212.7	11.48	5.92	33.5		24.6
25							354.5	11.72	12.6	15.4		11.3
50							709.0	12.06	35.8	5.47		4.03
150							2127	12.63	195	1.10		.809

<sup>a</sup>Droplet temperatures and evaporation rates not quantitative for calculated droplet temperatures higher than about 15° C.  
Evaporation rates omitted for droplet temperatures greater than 25° C.

TABLE II - Continued. RESULTS

(d) Temperature effects.

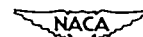


D <sub>d</sub> , microns	Altitude, ft	t <sub>d,∞</sub> , °C	M <sub>∞</sub>	M <sub>R</sub>	M <sub>T</sub>	V <sub>r</sub> , ft/sec	Re <sub>r</sub>	t <sub>d,s</sub> , °C	Q <sub>m</sub> , g/sec	Δ, fractional mass/sec	U <sub>1</sub> + V <sub>r</sub> , ft/sec	Q, fractional mass/ft
15	10,000	-30	0.75	0	0.063	68.14	22.76	-7.75	8.65×10 <sup>-9</sup>	4.88	68.14	71.6×10 <sup>-3</sup>
		-25				68.83	22.32	-5.86	11.5	6.53	68.83	94.9
		-20				69.52	21.93	-3.03	14.5	8.22	69.52	118
		-15				70.18	21.57	-3.93	17.6	9.98	70.18	142
		-10				70.90	21.23	-7.82	20.8	11.8	70.90	166
		-5				71.59	20.93	12.04	23.5	13.3	71.59	186
		-30			.25	270.3	89.58	-5.78	15.8	8.94	270.3	33.1
		-25				273.1	87.95	-1.96	20.8	11.8	273.1	43.2
		-20				275.9	86.36	1.92	25.9	14.7	275.9	53.2
		-15				278.5	84.95	5.79	31.1	17.6	278.5	63.2
		-10				281.3	83.63	9.69	36.4	20.6	281.3	73.2
		-5				284.0	82.44	13.91	40.8	23.1	284.0	81.4
		-30			.75	811.0	250.2	9.18	5.89×10 <sup>-8</sup>	33.3	811.0	41.1
		-25				819.5	245.9	12.87	7.09	40.1	819.5	48.9
		-20				827.7	241.7	16.68	8.25	46.7	827.7	56.4
		-15				835.6	237.6	20.58	9.38	53.1	835.6	63.5
		-10				844.1	233.9	24.59	10.5	59.5	844.1	70.5
		-5				852.0	230.7	28.98			852.0	
		-30			.25	0	0	-10.09	3.66×10 <sup>-9</sup>	2.07	268.8	7.70
		-25						-5.98	4.98	2.82	271.5	10.4
		-20						-1.96	6.43	3.64	274.3	13.3
		-15						2.05	7.99	4.52	276.9	16.3
		-10						6.01	9.60	5.43	279.6	19.4
		-5						10.26	11.0	6.22	282.2	22.1
		-30			.063	67.75	22.16	-10.18	7.00	3.96	336.8	11.8
		-25				68.40	21.74	-6.11	9.43	5.34	339.9	15.7
		-20				69.13	21.36	-2.12	12.1	6.83	343.4	19.9
		-15				69.78	20.99	1.84	14.8	8.39	346.7	24.2
		-10				70.47	20.66	5.77	17.7	10.0	350.2	28.6
		-5				71.13	20.36	10.02	20.1	11.4	353.4	32.3
		-30			.25	268.8	87.20	-8.11	12.6	7.15	537.7	13.3
		-25				271.5	85.50	-4.21	17.2	9.73	543.0	17.9
		-20				274.3	84.00	-2.27	21.7	12.3	548.5	22.4
		-15				276.9	82.69	3.66	26.4	14.9	553.8	27.0
		-10				279.6	81.26	7.59	31.2	17.7	559.4	31.6
		-5				282.2	80.15	11.83	35.3	20.0	564.6	35.4
		-30			.75	806.4	243.5	6.80	51.6	29.2	1075	27.1
		-25				814.7	239.0	10.52	62.7	35.5	1086	32.7
		-20				822.6	234.8	14.33	73.6	41.6	1097	38.0
		-15				830.7	230.9	18.23	84.3	47.7	1108	43.0
		-10				838.9	227.3	22.21	94.8	53.6	1118	48.0
		-5				846.8	224.1	26.58			1129	
		-30			.50	0	0	-17.56	1.76	.995	527.9	1.88
		-25						-13.11	2.52	1.43	533.1	2.68
		-20						-8.50	3.19	1.81	538.4	3.35
		-15						-4.24	4.18	2.36	543.6	4.35
		-10						-0.07	5.31	3.00	549.2	5.47
		-5						4.32	6.28	3.55	554.1	6.41
		-30			.063	66.50	20.43	-17.56	3.31	1.87	594.4	3.15
		-25				67.16	20.03	-13.13	4.71	2.67	600.3	4.44
		-20				67.85	19.68	-8.55	5.91	3.34	606.6	5.51
		-15				68.50	19.32	-4.31	7.66	4.34	612.1	7.08
		-10				69.19	19.04	-1.16	9.65	5.46	618.4	8.83
		-5				69.85	18.77	4.20	11.3	6.39	624.3	10.2
		-30			.25	263.9	80.39	-15.54	6.41	3.63	791.7	4.58
		-25				266.5	78.83	-11.14	8.83	5.00	799.5	6.25
		-20				269.2	77.48	-6.76	11.3	6.41	807.7	7.94
		-15				271.8	76.10	-2.55	14.4	8.17	815.6	10.0
		-10				274.6	74.90	1.53	17.8	10.1	823.8	12.2
		-5				277.1	73.85	5.87	20.7	11.7	831.4	14.1
		-30			.75	791.7	224.3	-0.08	32.9	18.9	1320	14.1
		-25				799.6	220.2	3.70	41.8	23.6	1333	17.7
		-20				807.7	216.3	7.56	50.5	28.6	1346	21.2
		-15				815.6	212.7	11.48	59.2	33.5	1359	24.6
		-10				823.8	209.4	15.45	67.8	38.4	1373	27.9
		-5				831.4	206.6	19.77	75.1	42.5	1385	30.7

<sup>a</sup>Droplet temperatures and evaporation rates not quantitative for calculated droplet temperatures higher than about 15° C. Evaporation rates omitted for droplet temperatures greater than 25° C.

TABLE II - Continued. RESULTS

(e) Altitude effects.



$D_d$ , microns	Altitude, ft	$t_{d,c}$ , °C	$M_\infty$	$M_R$	$M_T$	$V_R$ , ft/sec	$Re_R$	$t_{d,s}$ , °C	$Q_{ev}$ , g/sec	$\Lambda$ , fractional mass/sec	$U_1 + V_R$ , ft/sec	$\Omega$ , fractional mass/ft
15	3,000	-25	0.75	0	0.063	68.83	29.58	-2.74	$10.6 \times 10^{-9}$	5.98	68.83	$86.8 \times 10^{-5}$
	6,000						26.21	-3.22		11.0		90.3
	10,000						22.32	-3.86		11.5		94.9
	15,000						18.53	-4.64		12.2		100
	22,500						14.11	-5.83		15.2		108
	30,000						11.08	-6.93		14.0		115
	3,000				.25	273.1	116.4	-1.70	19.7	11.2	273.1	40.8
	6,000						103.2	-1.24	20.2	11.4		41.8
	10,000						87.93	-1.96	20.8	11.8		45.2
	15,000						72.95	-2.83	21.5	12.2		44.6
	22,500						55.56	-4.17	22.4	12.7		46.4
	30,000						43.64	-5.39	23.0	13.0		47.7
	3,000				.75	819.5	325.7	15.16	69.3	39.2		47.8
	6,000						288.3	14.19	70.0	39.6		48.4
	10,000						245.9	12.87	70.9	40.1		48.9
	15,000						204.0	11.29	71.5	40.5		49.4
	22,500						165.3	8.910	71.6	40.5		49.5
	30,000						122.0	6.805	71.3	40.3		49.2
	3,000			.25	0	0	0	-5.06	4.16	2.55	271.5	8.66
	6,000							-5.45	4.50	2.55		9.58
	10,000							-5.98	4.98	2.82		10.4
	15,000							-6.64	5.58	3.15		11.6
	22,500							-7.65	6.51	3.68		13.6
	30,000							-8.56	7.33	4.15		15.3
	3,000				.063	68.40	28.80	-5.15	8.55	4.84	339.9	14.2
	6,000						25.52	-5.56	8.92	5.05		14.9
	10,000						21.74	-6.11	9.43	5.34		15.7
	15,000						18.05	-6.80	10.0	5.66		16.7
	22,500						13.74	-7.85	10.9	6.15		18.1
	30,000						10.79	-8.79	11.6	6.66		19.5
	3,000				.25	271.5	113.3	-3.14	16.1	9.12	543.0	16.8
	6,000						100.4	-3.57	16.6	9.40		17.3
	10,000						85.50	-4.21	17.2	9.73		17.9
	15,000						70.95	-4.99	17.8	10.1		18.6
	22,500						54.05	-6.18	18.7	10.6		19.5
	30,000						42.45	-7.28	19.3	10.9		20.1
	3,000				.75	814.7	316.7	12.61	61.1	34.6	1086	31.8
	6,000						280.7	11.75	61.9	35.0		32.5
	10,000						239.0	10.52	62.7	35.5		32.7
	15,000						198.3	9.04	63.3	35.8		33.0
	22,500						151.1	6.86	63.7	36.0		33.2
	30,000						118.7	4.90	63.6	35.9		33.1
	3,000			.50	0	0	0	-12.57	2.05	1.16	533.1	2.17
	6,000							-12.80	2.24	1.27		2.38
	10,000							-13.11	2.52	1.43		2.68
	15,000							-13.51	2.88	1.63		3.05
	22,500							-14.17	3.43	1.94		3.64
	30,000							-14.78	3.98	2.25		4.25
	3,000				.063	67.16	26.52	-12.63	4.11	2.52	600.3	3.87
	6,000						23.51	-12.80	4.38	2.48		4.13
	10,000						20.03	-13.13	4.71	2.67		4.44
	15,000						16.62	-13.57	5.10	2.89		4.81
	22,500						12.66	-14.23	5.70	3.23		5.38
	30,000						9.939	-14.89	6.21	3.51		5.85
	3,000				.25	266.5	104.4	-10.48	8.02	4.54	799.5	5.67
	6,000						92.43	-10.75	8.37	4.73		5.92
	10,000						78.83	-11.14	8.83	5.00		6.25
	15,000						65.37	-11.65	9.35	5.29		6.62
	22,500						49.80	-12.45	10.1	5.72		7.15
	30,000						39.12	-13.23	10.7	6.05		7.57
	3,000				.75	799.6	291.5	5.29	40.3	22.8	1333	17.1
	6,000						238.2	4.61	41.0	23.2		17.4
	10,000						220.2	3.70	41.8	23.6		17.7
	15,000						182.6	2.58	42.4	24.0		18.0
	22,500						159.1	.91	43.1	24.4		18.5
	30,000						109.2	-.61	43.4	24.5		18.4

<sup>a</sup>Droplet temperatures and evaporation rates not quantitative for calculated droplet temperatures higher than about 15° C.  
Evaporation rates omitted for droplet temperatures greater than 25° C.



TABLE II - Concluded. RESULTS

(f) Relative humidity effects.



$D_d$ , microns	Altitude, ft	$t_{at, \infty}$ , °C	$M_\infty$	$M_R$	$M_T$	$V_r$ , ft/sec	$Re_r$	$\sigma$	$t_{d, s}$ , °C	$Q_m$ , g/sec	$\Lambda$ , fractional mass/sec	$U_1 + V_r$ , ft/sec	$\Omega$ , fractional mass/ft
15	10,000	-25	0.75	0	0.083	68.85	22.32	0.9 1.00	-4.00 -3.86	$11.8 \times 10^{-9}$ 11.5	6.65 6.53	68.85	$96.7 \times 10^{-3}$ 94.9
					.25	27.51	87.86	.9 1.00	-2.08 -1.96	21.2 20.8	12.0 11.8	273.1	43.9 43.2
					.75	819.5	245.9	.9 1.00	12.77 12.87	71.4 70.9	40.4 40.1	819.5	49.3 48.9
					.25 0	0	0	.9 1.00	-6.12 -5.98	5.10 4.98	2.88 2.82	271.5	10.6 10.4
					.063	68.40	21.74	.9 1.00	-6.25 -6.11	9.66 9.43	5.46 5.34	339.9	16.1 15.7
					.25	271.5	855.0	.9 1.00	-4.35 -4.21	17.5 17.2	9.91 9.73	543.0	18.3 17.9
					.75	814.7	239.0	.9 1.00	10.40 10.52	63.2 62.7	35.8 35.5	1086	32.9 32.7
					.50 0	0	0	.9 1.00	-13.27 -13.11	2.65 2.52	1.50 1.43	533.1	2.82 2.69
					.063	67.16	20.03	.9 1.00	-13.30 -13.13	4.96 4.71	2.61 2.67	600.3	4.68 4.44
					.25	266.5	78.83	.9 1.00	-11.30 -11.14	9.21 8.83	5.21 5.00	799.5	6.52 6.25
					.75	799.6	220.2	.9 1.00	3.57 3.70	42.2 41.8	23.9 23.6	1333	17.9 17.7

TABLE III. - AMBIENT CONDITIONS OF CALCULATIONS

[Pressures from Signal Corp. RAOB chart (ML-248)  
for particular temperatures and altitudes]

Altitude, ft	Flight air temperature, °C	Air pressure	
		dyne cm <sup>-2</sup>	atm
3,000	-30	8.925X10 <sup>5</sup>	0.8808
	-25	8.94	.8823
	-20	8.96	.8843
	-15	8.98	.8863
	-10	8.995	.8877
	-5	9.015	.8897
6,000	-30	7.89	0.7787
	-25	7.92	.7816
	-20	7.955	.7851
	-15	7.995	.7890
	-10	8.025	.7920
	-5	8.06	.7955
10,000	-30	6.70	0.6612
	-25	6.75	.6662
	-20	6.80	.6711
	-15	6.85	.6760
	-10	6.905	.6815
	-5	6.97	.6879
15,000	-30	5.54	0.5468
	-25	5.60	.5528
	-20	5.66	.5586
	-15	5.72	.5645
	-10	5.79	.5714
	-5	5.86	.5783
22,500	-30	4.185	0.4130
	-25	4.265	.4209
	-20	4.345	.4288
	-15	4.42	.4362
	-10	4.50	.4441
	-5	4.59	.4530
30,000	-30	3.26	0.3217
	-25	3.35	.3306
	-20	3.44	.3395
	-15	3.53	.3484
	-10	3.625	.3578
	-5	3.725	.3676



2734

CJ-6

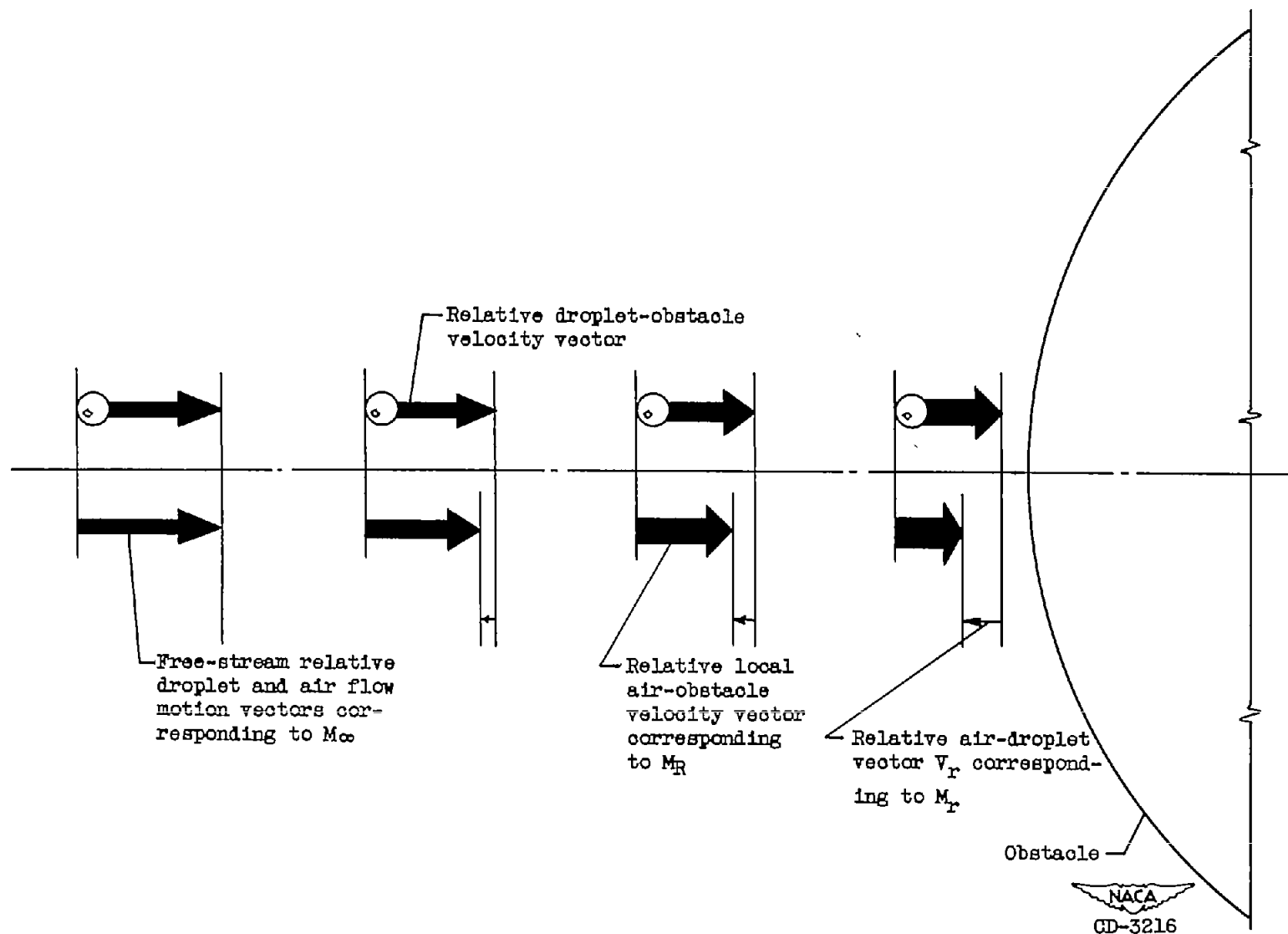


Figure 1. - Motional relations among air-stream, droplet, and obstacle.

2734

CJ-6 back

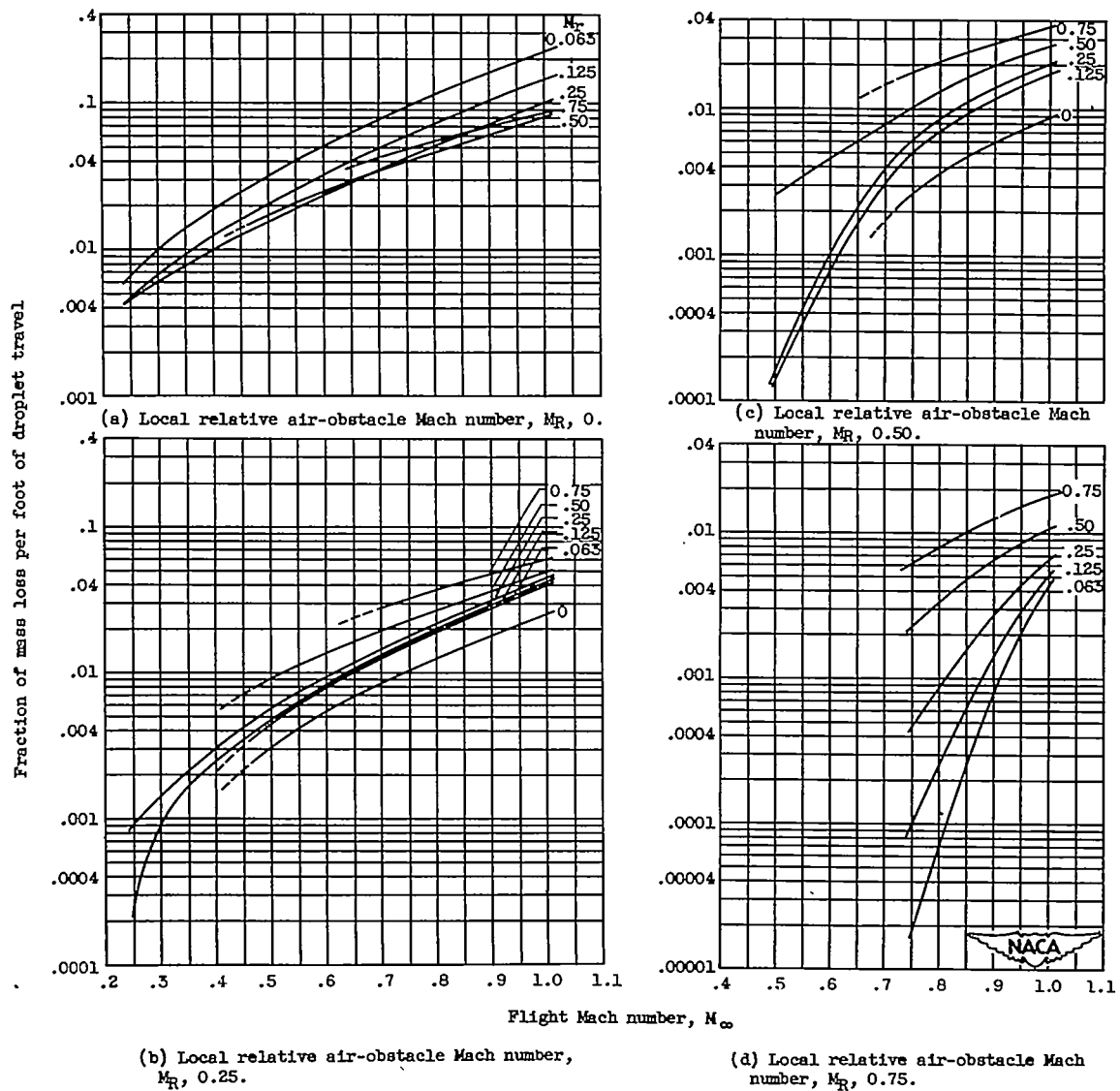


Figure 2. - Variation of mass loss rate with flight Mach number. Altitude, 10,000 feet; ambient temperature,  $-25^\circ\text{C}$ ; droplet diameter, 15 microns.

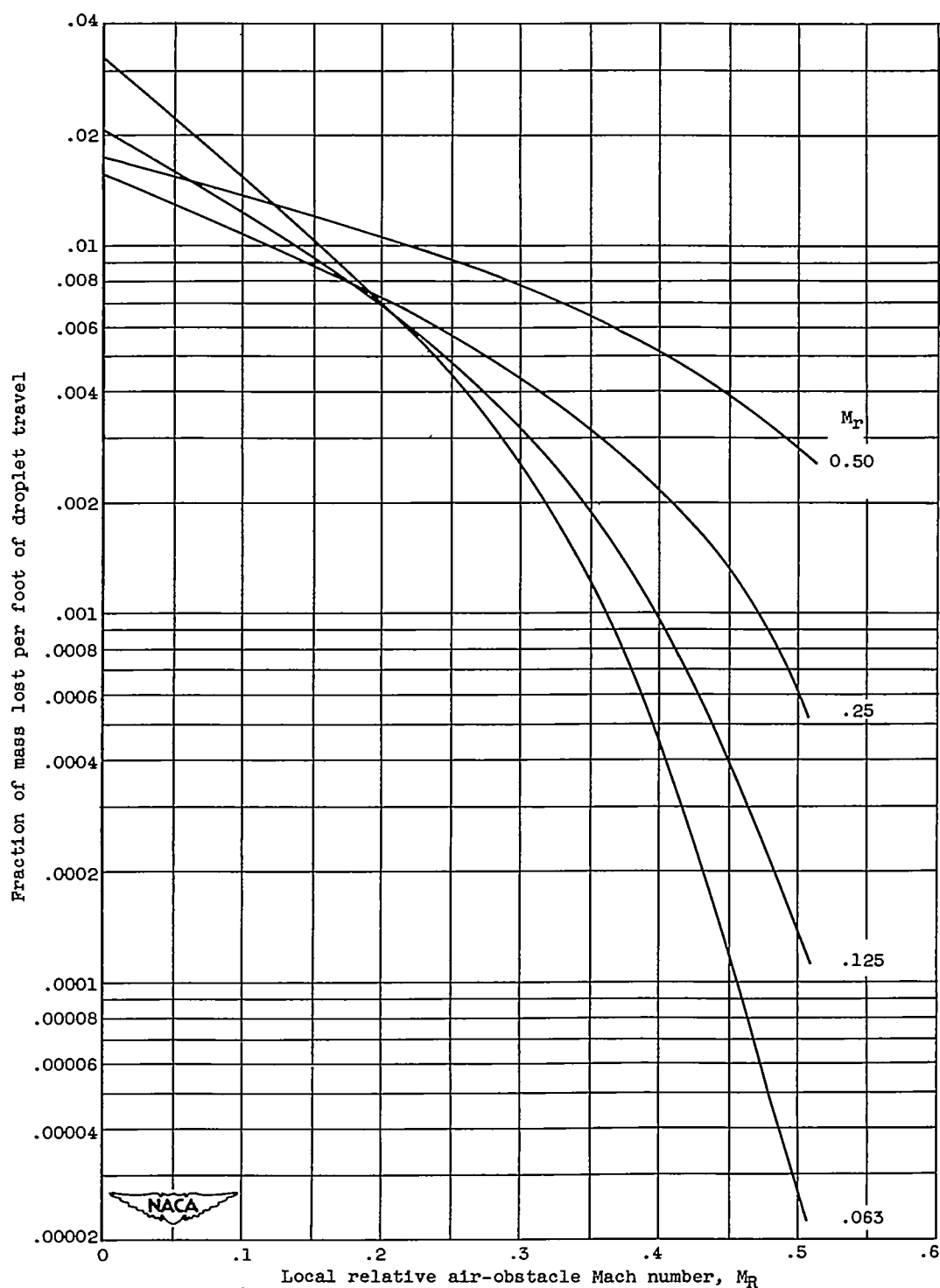
(a) Flight Mach number,  $M_\infty$ , 0.50.

Figure 3. - Variation of mass loss rate with relative air-obstacle Mach number.  
 Altitude, 10,000 feet; ambient temperature,  $-25^\circ\text{C}$ ; droplet diameter,  
 15 microns.

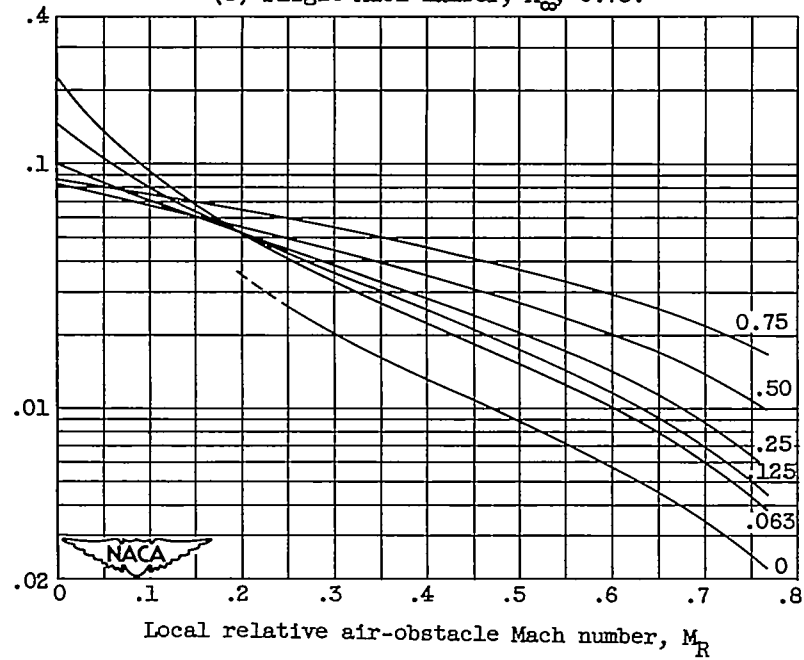
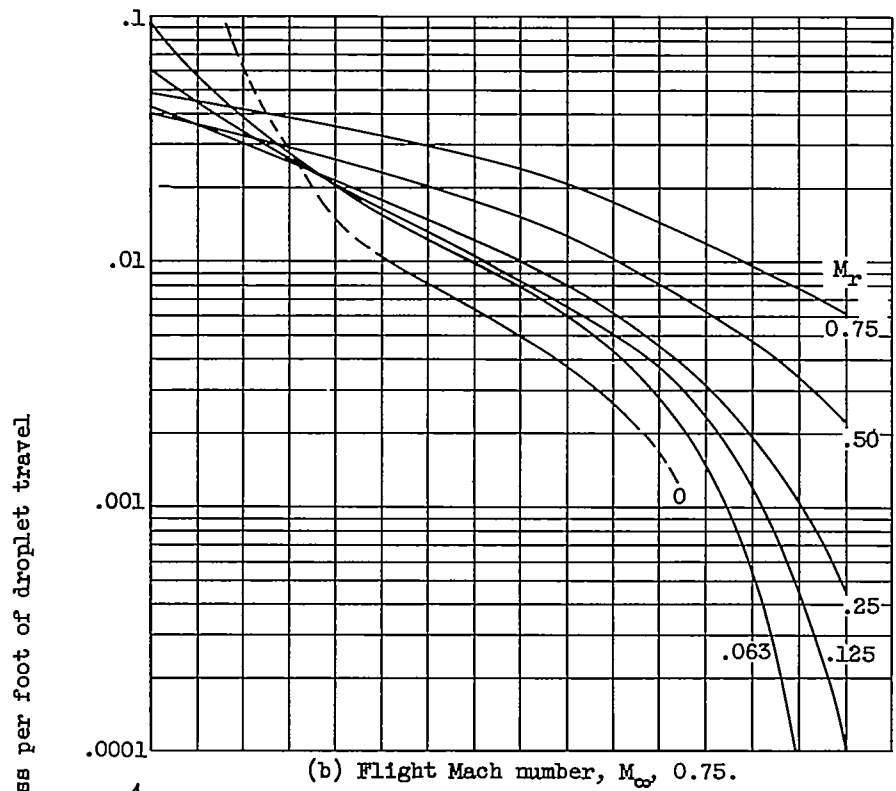
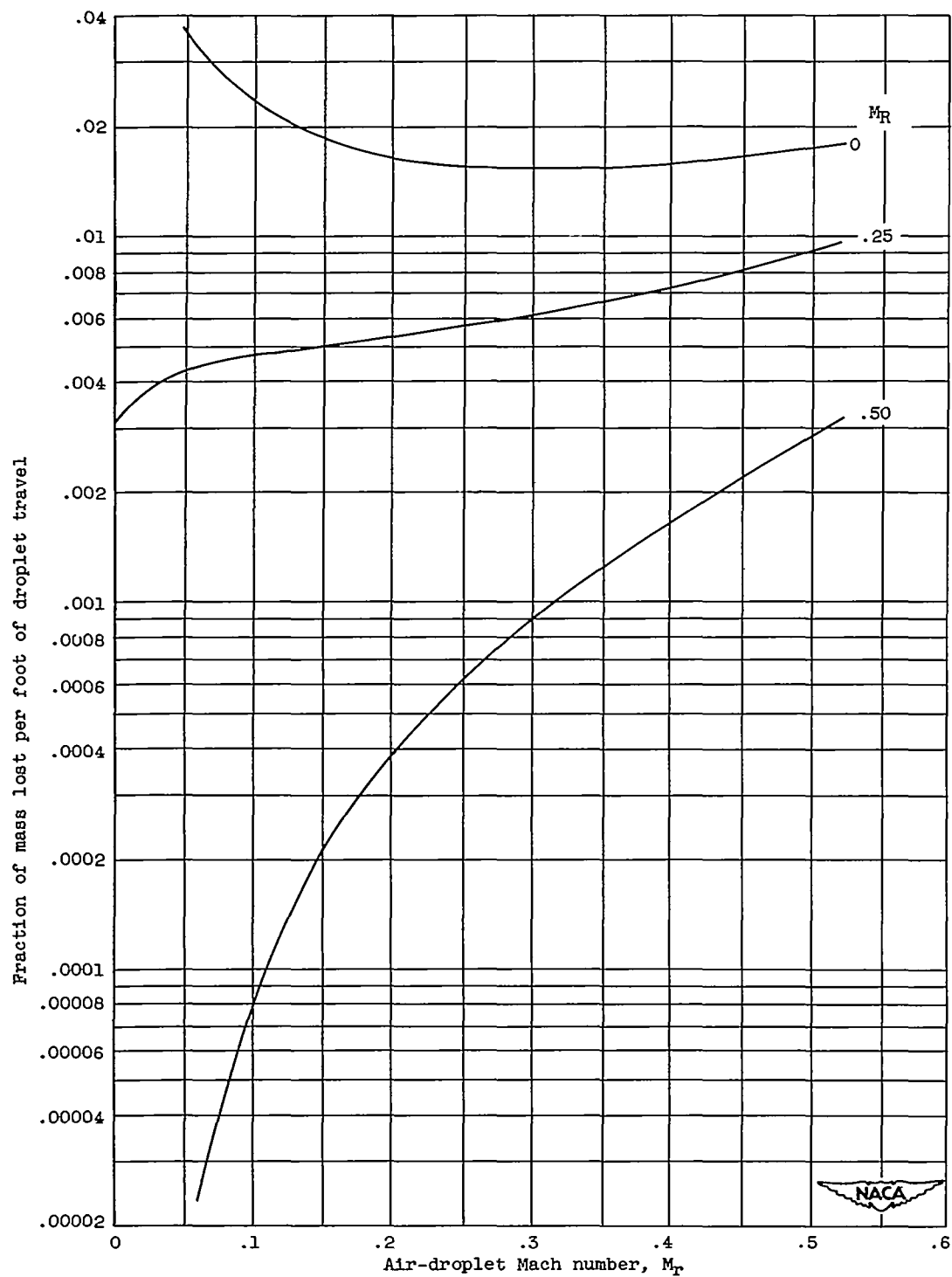


Figure 3. - Concluded. Variation of mass loss rate with relative air-obstacle Mach number. Altitude, 10,000 feet; ambient temperature,  $-25^\circ\text{C}$ ; droplet diameter, 15 microns.



(a) Flight Mach number,  $M_\infty$ , 0.50.

Figure 4. - Variation of mass loss rate with relative air-droplet Mach number. Altitude, 10,000 feet; ambient temperature, 25° C; droplet diameter, 15 microns.

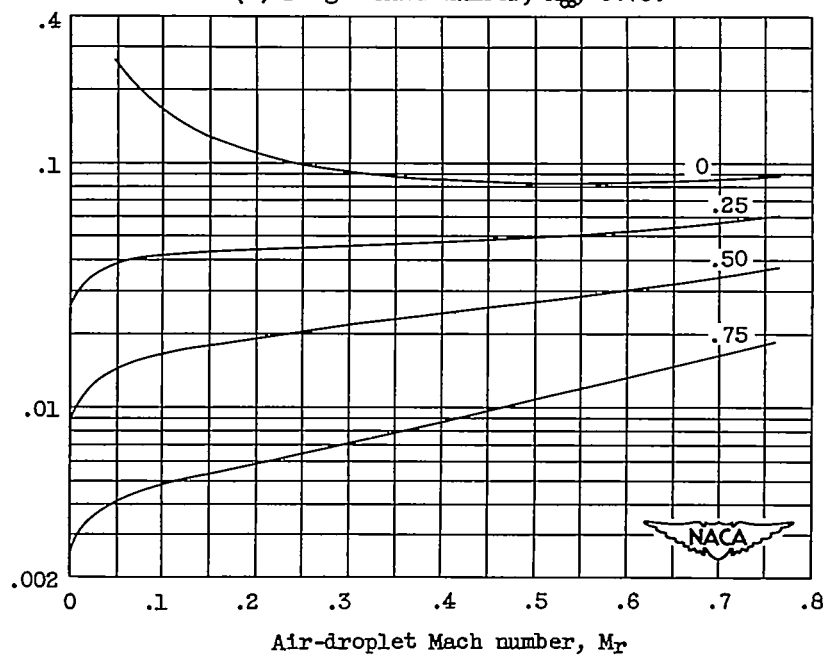
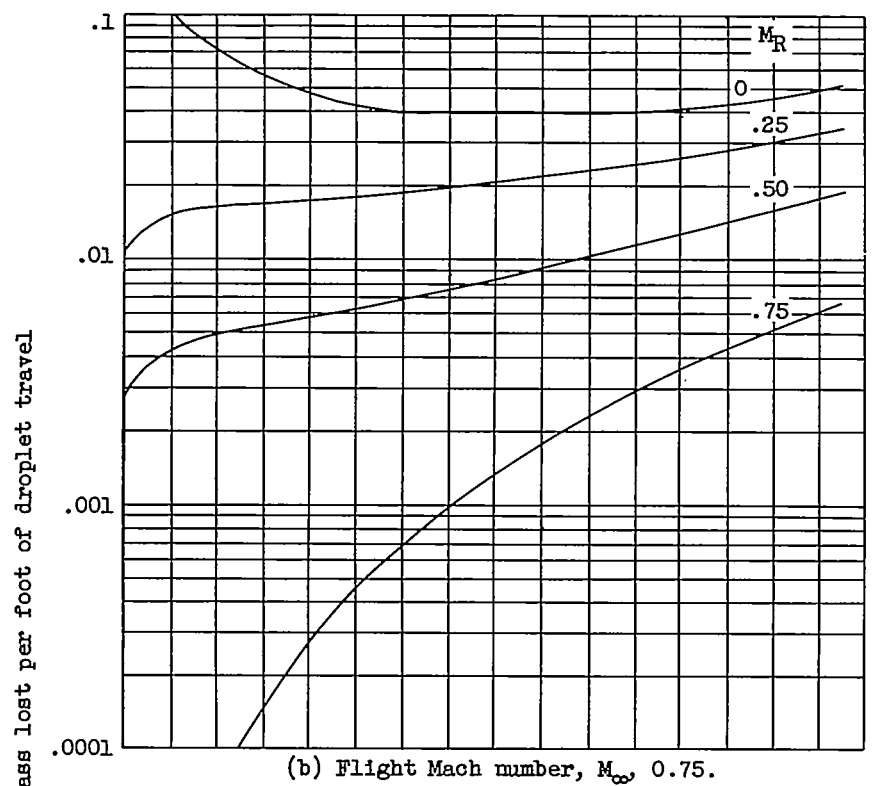


Figure 4. - Concluded. Variation of mass loss rate with relative air-droplet Mach number. Altitude, 10,000 feet; ambient temperature, 25° C; droplet diameter, 15 microns.



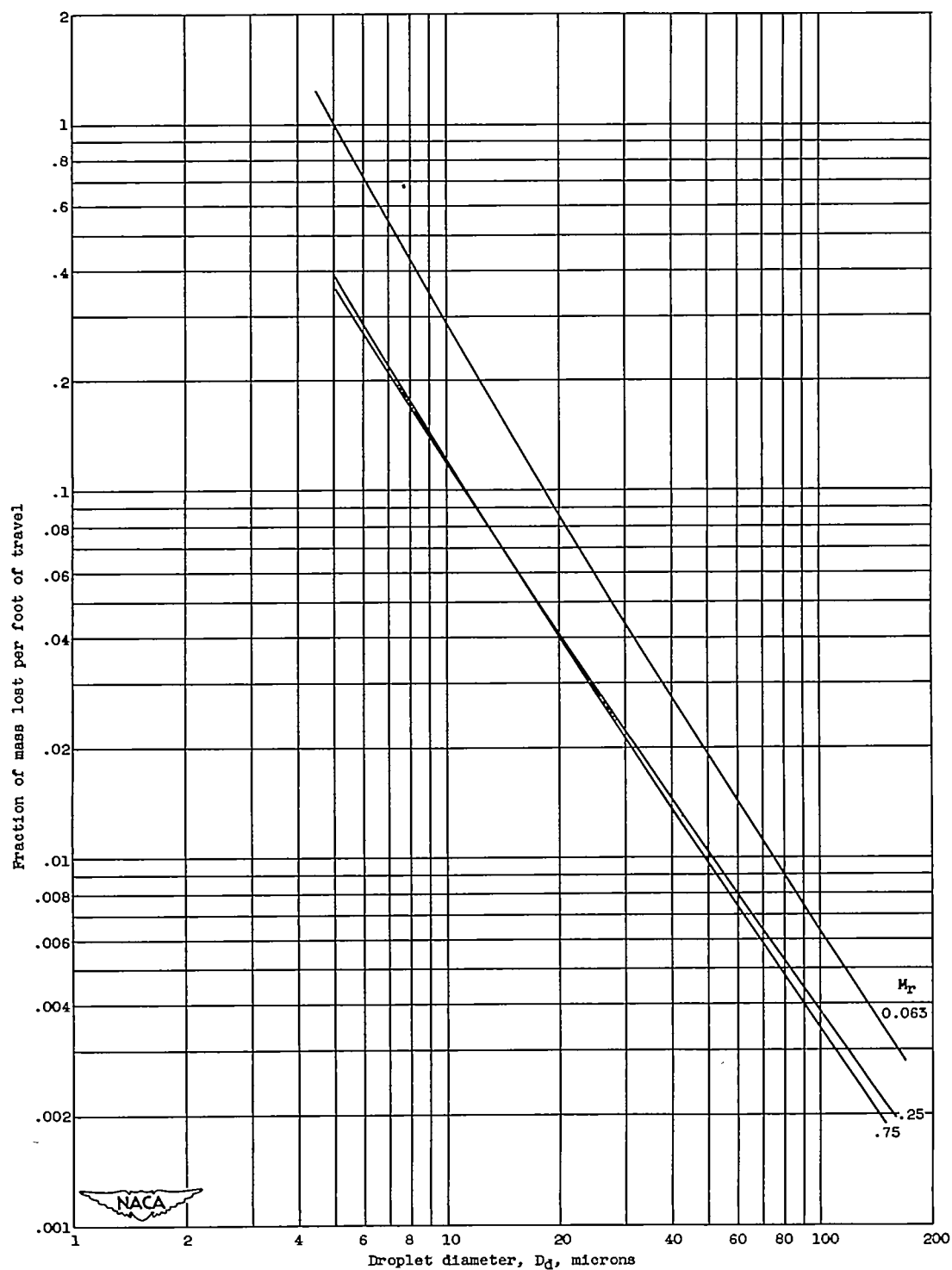
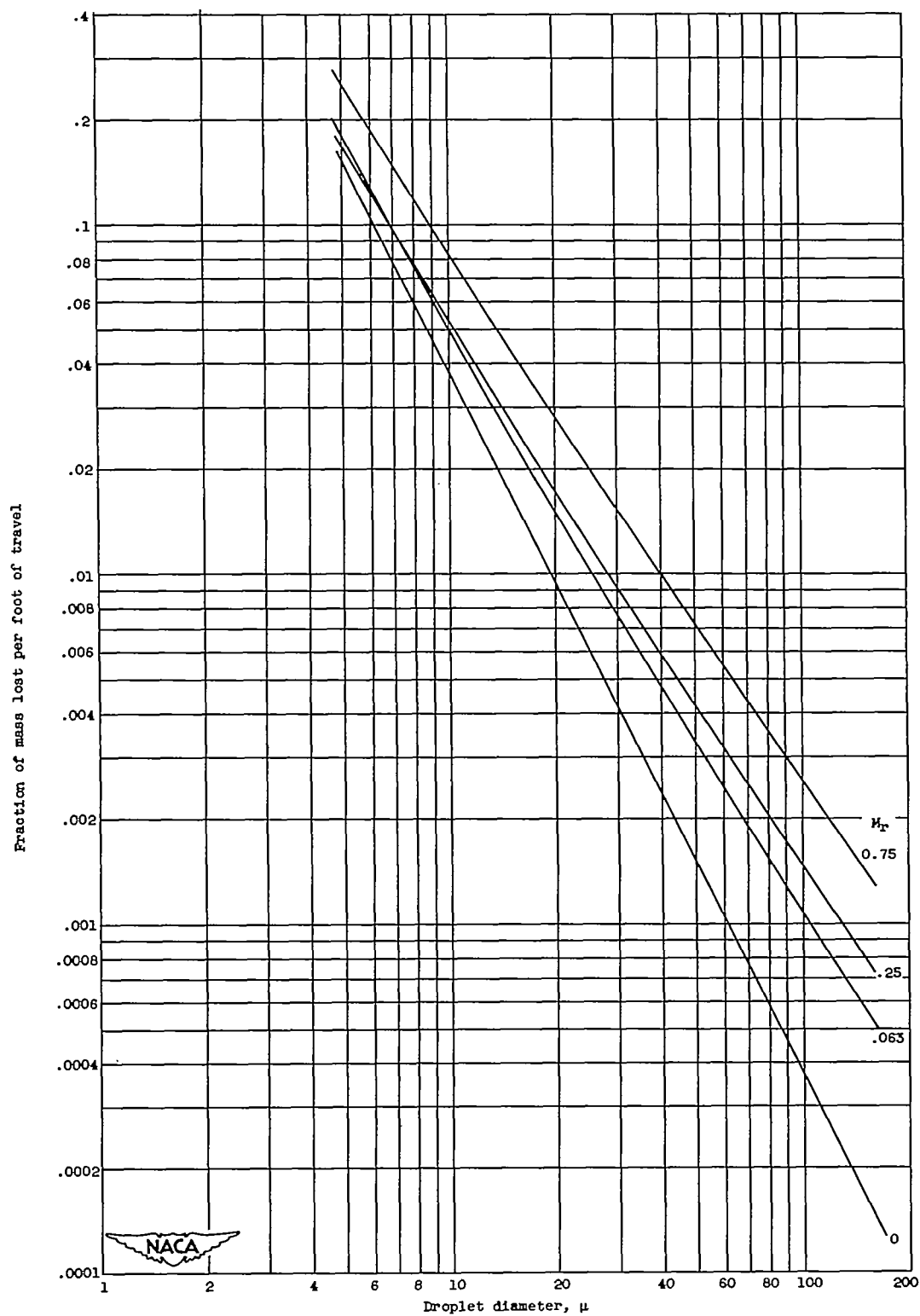
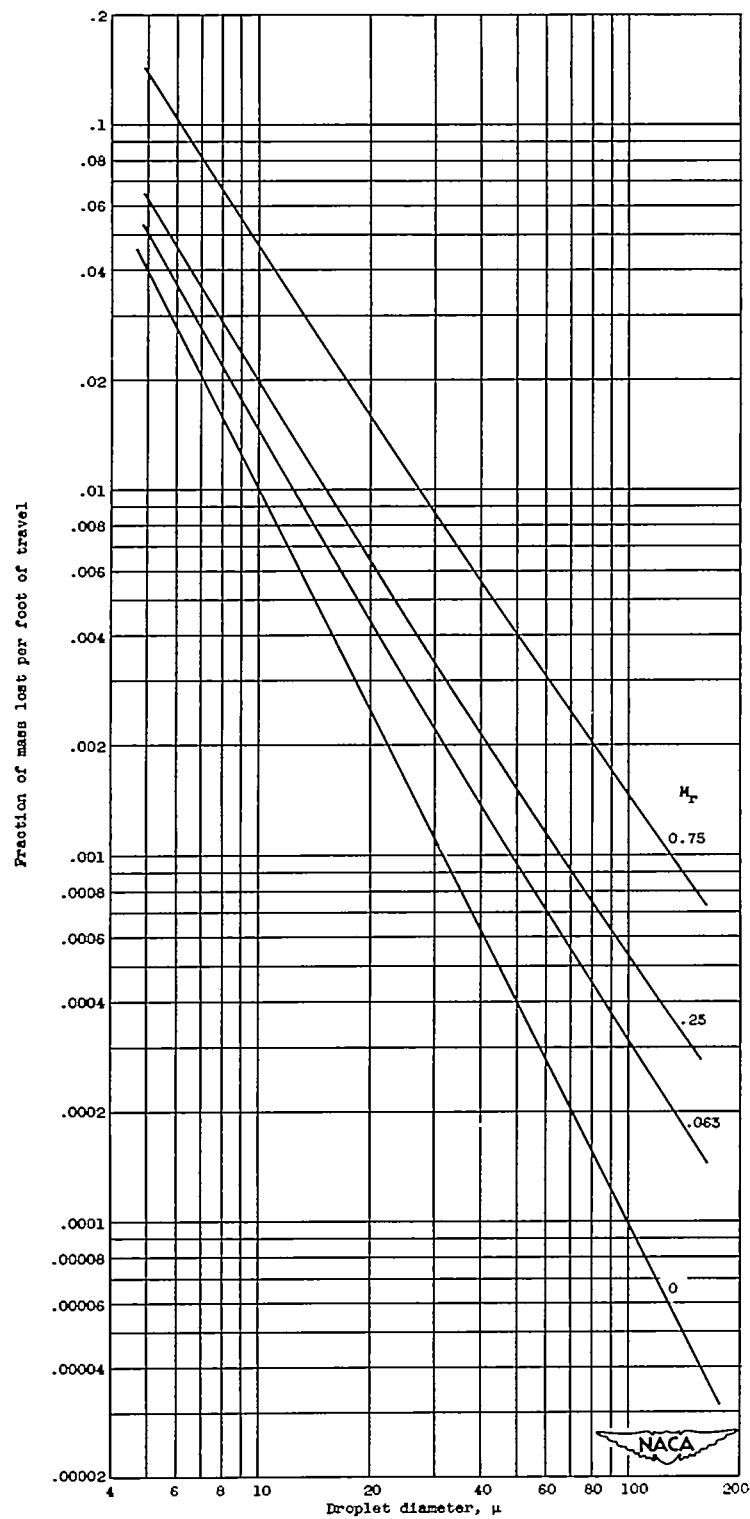
(a) Local relative air-obstacle Mach number,  $M_R$ , 0.

Figure 5. - Variation of mass-loss rate with droplet diameter. Altitude, 10,000 feet; ambient temperature, 15° C; flight Mach number, 0.75.



(b) Local relative air-obstacle Mach number,  $M_R$ , 0.25.

Figure 5. - Continued. Variation of mass-loss rate with droplet diameter. Altitude, 10,000 feet; ambient temperature, 15° C; flight Mach number, 0.75.



(c) Local relative air-obstacle Mach number,  $M_R$ , 0.50.

Figure 5. - Concluded. Variation of mass-loss rate with droplet diameter. Altitude, 10,000 feet; ambient temperature, 15° C; flight Mach number, 0.75.

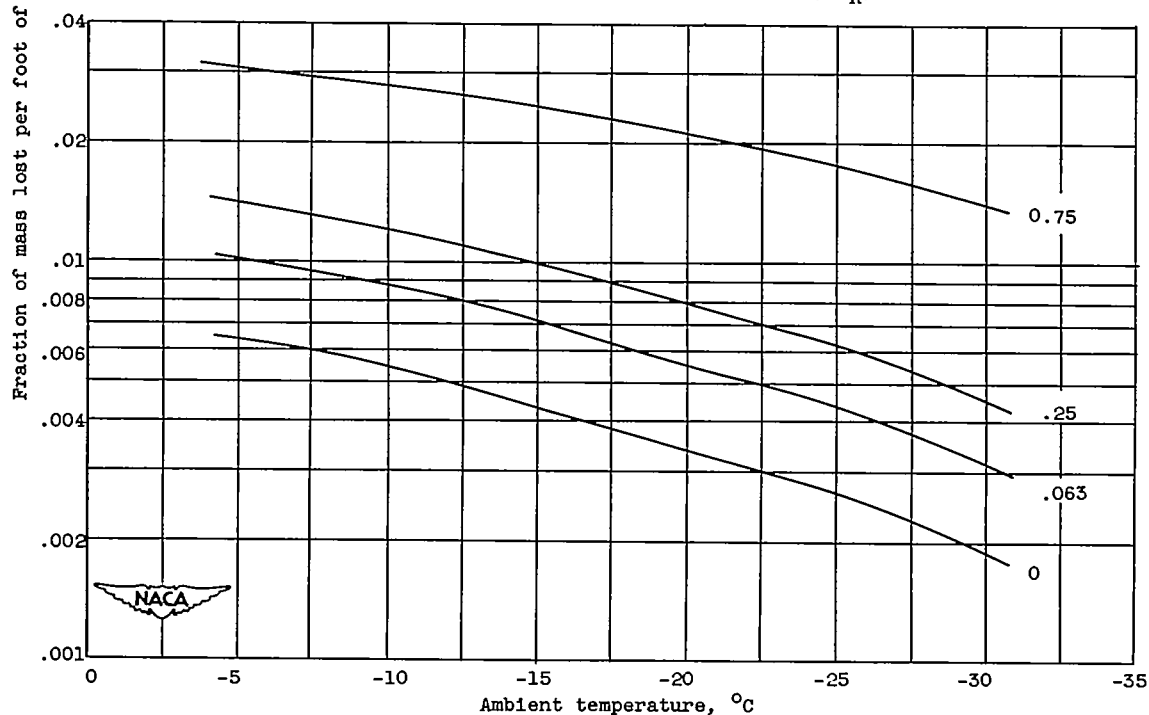
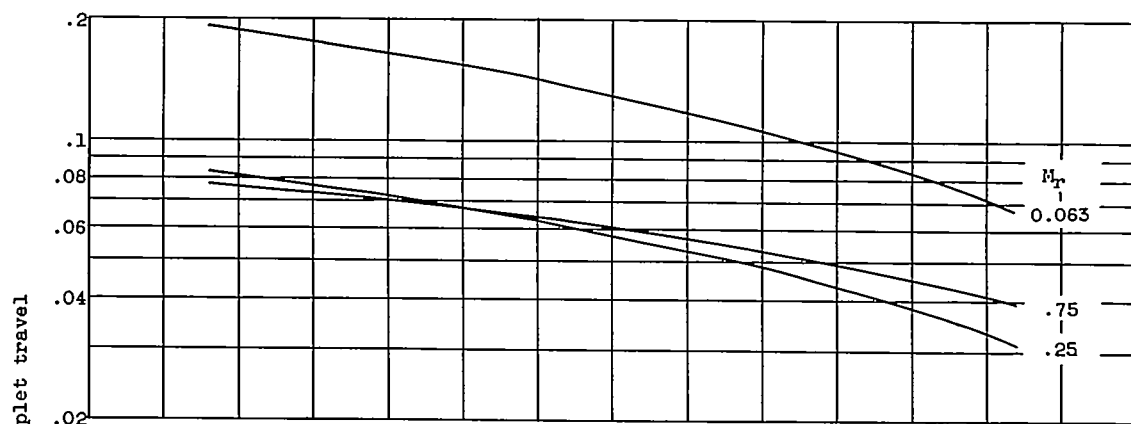


Figure 6. - Variation of mass-loss rate with ambient temperature. Altitude, 10,000 feet; droplet diameter, 15 microns; flight Mach number, 0.75.

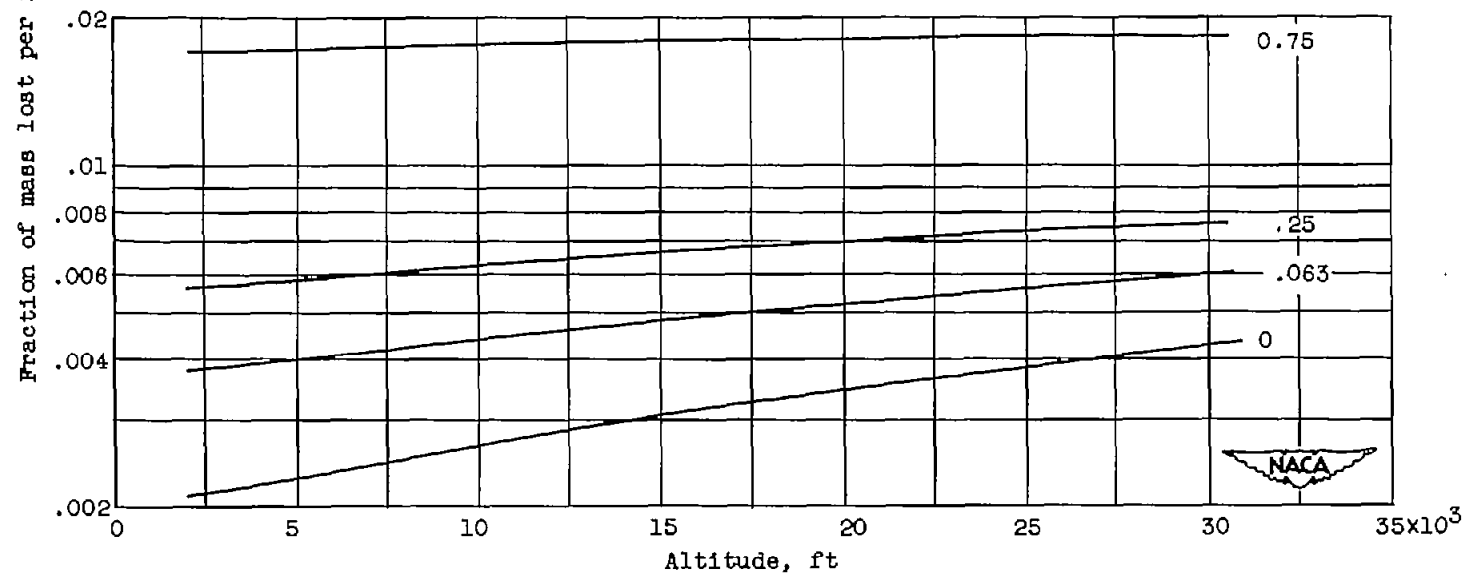
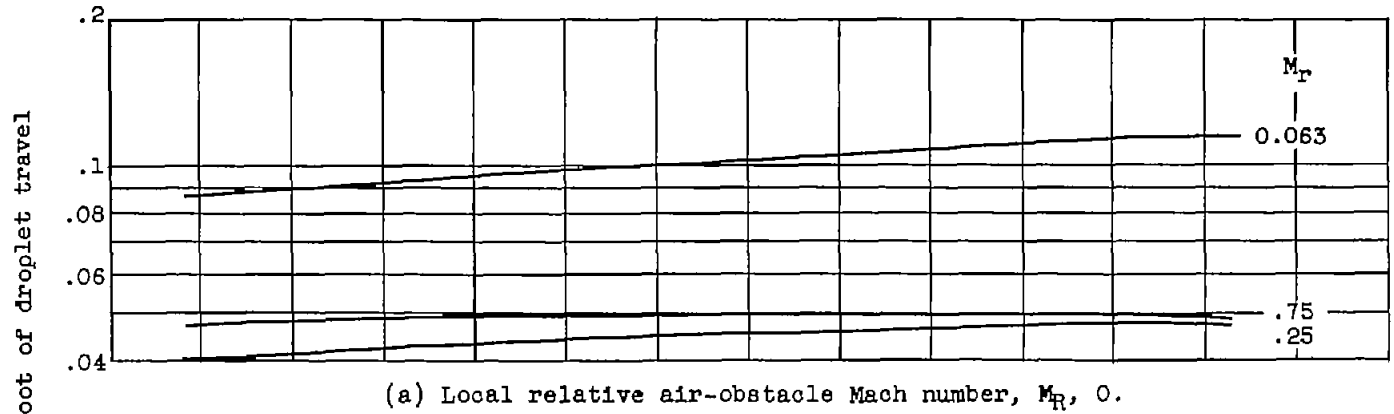


Figure 7. - Variation of mass-loss rate with altitude. Ambient temperature,  $-25^{\circ}\text{C}$ ; droplet diameter, 15 microns; flight Mach number, 0.75.

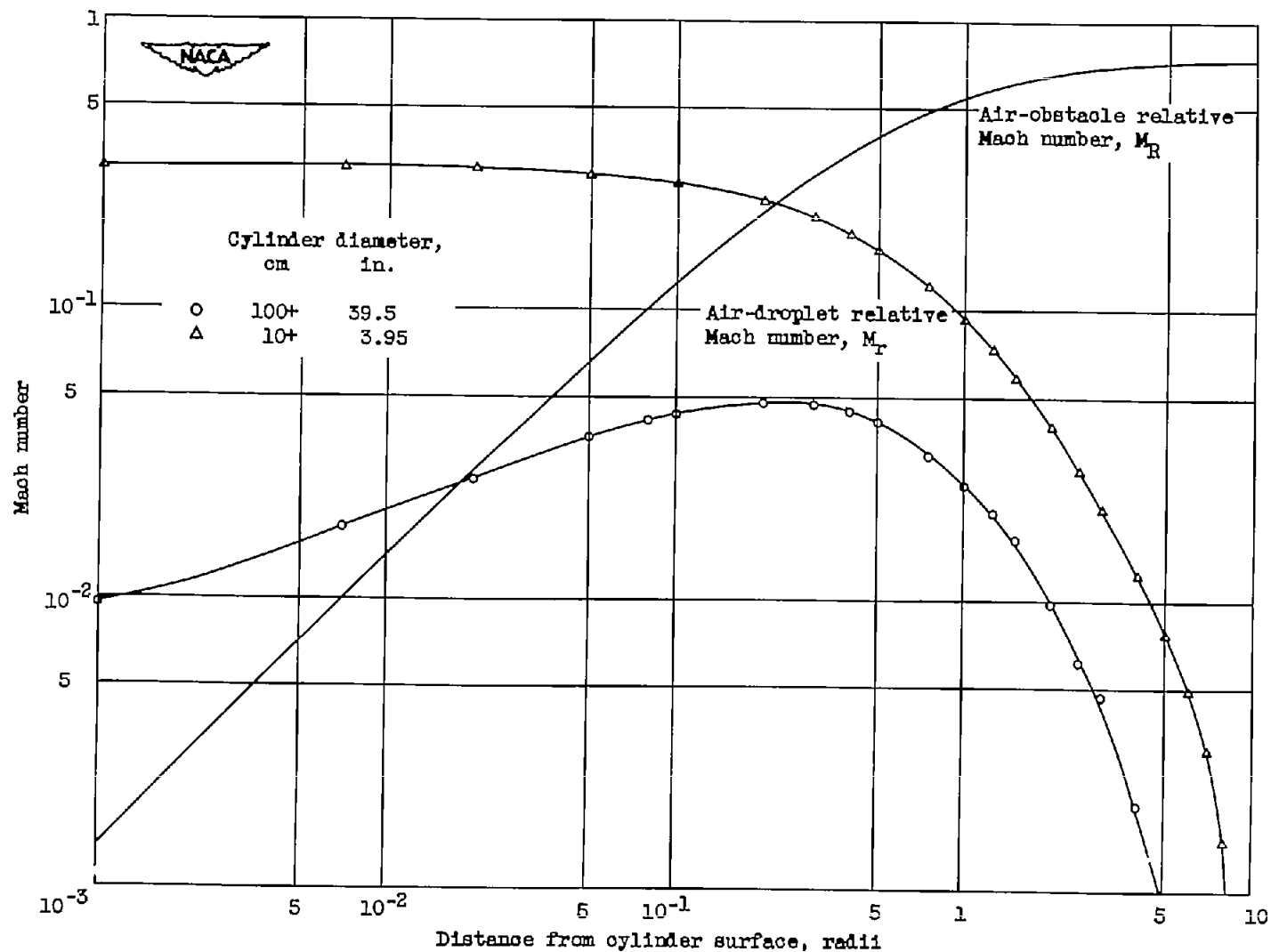


Figure 8. - Air and droplet speeds along stagnation lines ahead of circular cylinders. Altitude, 10,000 feet; ambient temperature,  $-25^{\circ}\text{C}$ ; droplet diameter, 15 microns; flight Mach number, 0.75.

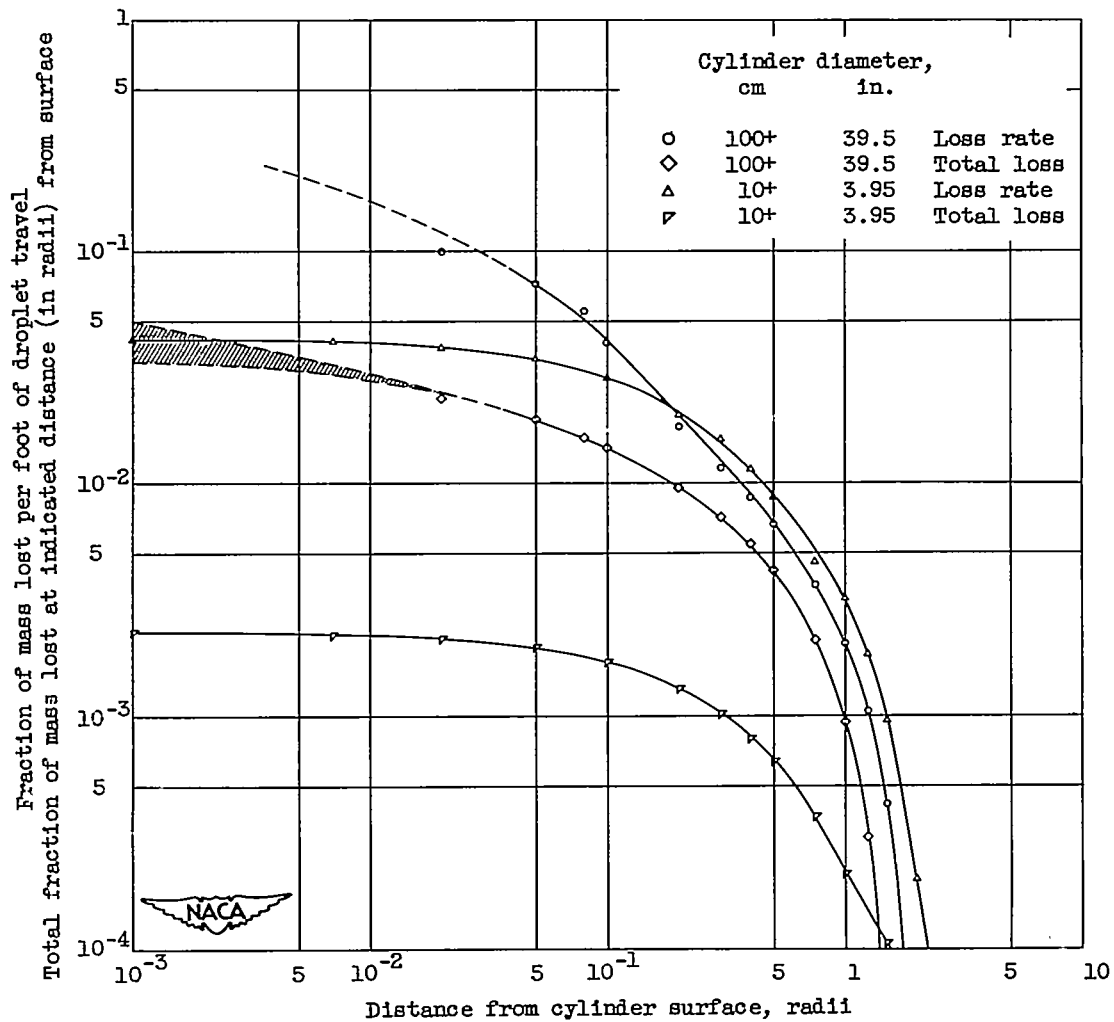


Figure 9. - Limiting mass losses from droplets impinging on circular cylinders.  
 Altitude, 10,000 feet; ambient temperature,  $-25^{\circ}\text{C}$ ; droplet diameter, 15 microns;  
 flight Mach number, 0.75.

2734

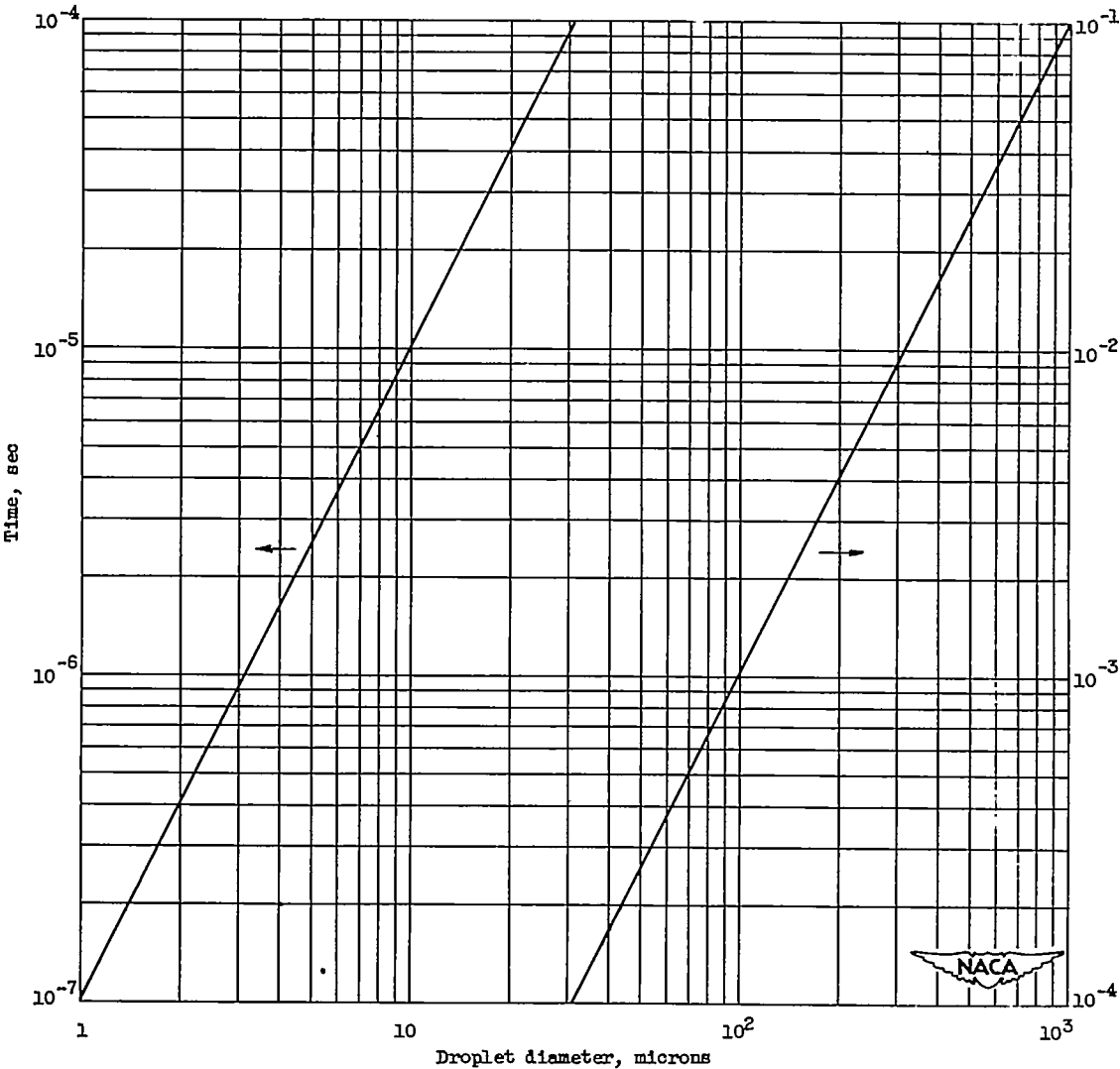


Figure 10. - Internal time-constant of water sphere.



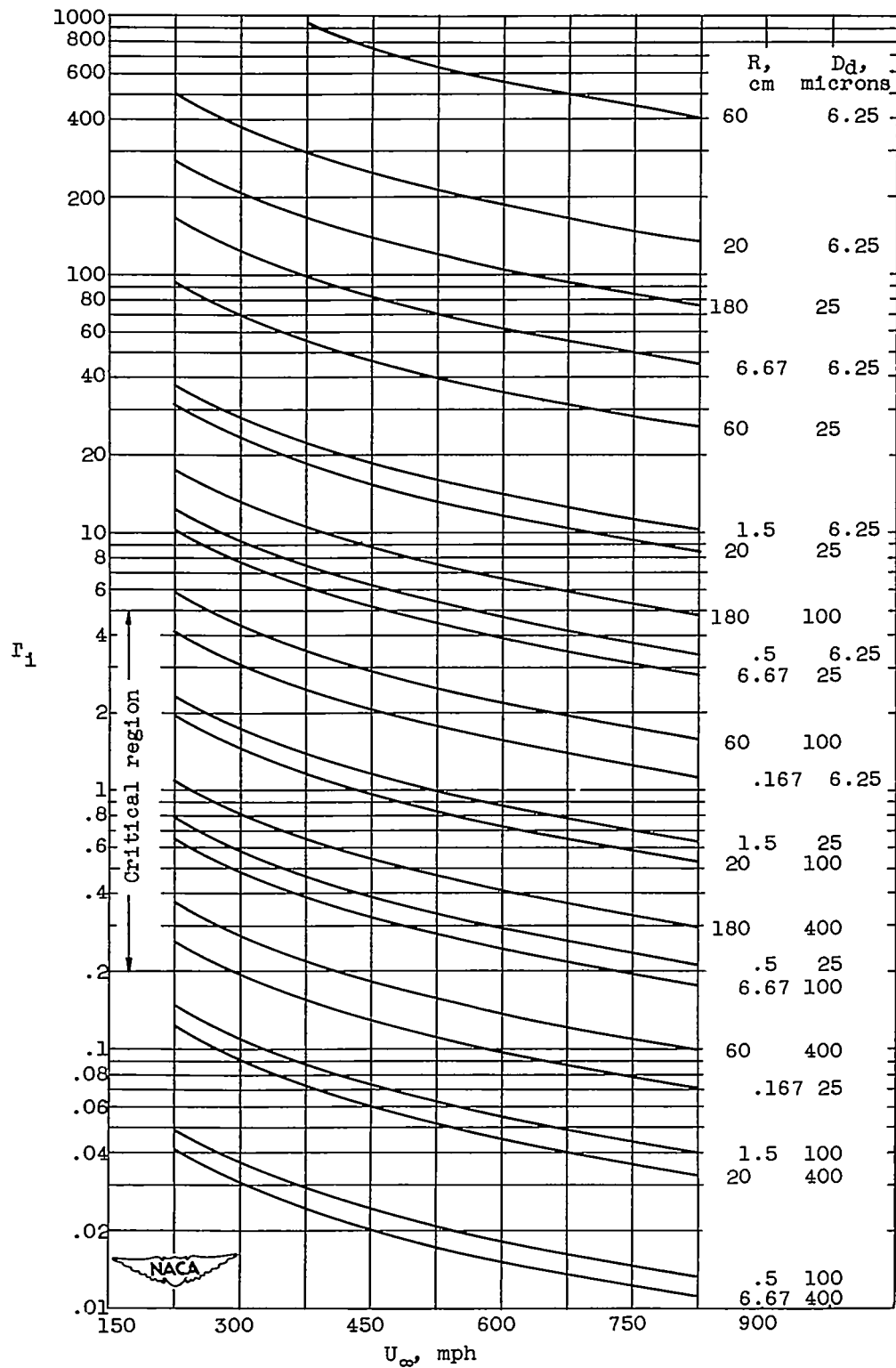


Figure 11. - Number of droplet internal response periods per approach period.